Electronic Supplementary Material (ESI) for Dalton Transactions.

Electronic Supporting Information

Synthesis, structures and cytotoxic effects *in vitro* of *cis*- and *trans*-[$Pt^{IV}Cl_4(NHC)_2$] complexes and their Pt^{II} precursors

Tobias Rehm,[a] Matthias Rothemund,[a] Thomas Dietel,[b] Rhett Kempe[b] and Rainer Schobert[a]

[a]*Organic Chemistry Laboratory, University Bayreuth, Universitaetsstrasse 30, 95440 Bayreuth, Germany. E-mail: Rainer.Schobert@uni-bayreuth.de*

[b]*Lehrstuhl fuer Anorganische Chemie II, University Bayreuth, Universitaetsstrasse 30, 95440 Bayreuth, Germany.*

Table of content

Table S 1: Single crystal X-ray diffraction data of platinum carbene complexes **2c** and **3**.

Crystal data	**2c**	**3**
Chemical formula	$C_{30}H_{44}Cl_2N_4Pt \cdot CHCl_3$	$C_{34}H_{32}Cl_4N_4Pt \cdot 2(CH_2Cl_2)$
M_r	846.07	983.87
Crystal system, space group	Triclinic, P	Monoclinic, C2/c
Temperature (K)	133	133
a, *b*, *c* (Å)	8.6162 (17), 12.200 (2), 17.892 (4)	24.684 (5), 8.277 (5), 22.505 (5)
α, β, γ (°)	104.49 (3), 95.13 (3), 104.88 (3)	121.662 (5)
V (Å^3)	1736.1 (7)	3914 (3)
Z	2	4
F(000)	842.5	1945
D_x (Mg m^{-3})	1.618	1.670
Radiation type	Mo Kα	Mo Kα
No. of reflections for cell measurement	1222	8743
θ range (°) for cell measurement	5.7–25.8	1.9–28.3
μ (mm^{-1})	4.45	3.81
Crystal shape	Block	Block
Colour	Clear colourless	Colourless
Crystal size (mm)	0.07 × 0.01 × 0.004	0.21 × 0.12 × 0.09
Data collection		
Diffractometer	STOE-STADIVARI	STOE-STADIVARI
Scan method	ω scans	ω scan
Absorption correction	Numerical	Numerical STOE-X-RED32
T_{min}, T_{max}	0.613, 0.733	0.841, 0.912
No. of measured, independent and observed [$I > 2\sigma(I)$] reflections	20838, 8234, 7605	10695, 3414, 2307
R_{int}	0.015	0.077
θ values (°)	θmax = 28.5, θmin = 1.8	θmax = 25.0, θmin = 2.0
$(\sin\theta/\lambda)_{max}$ (Å^{-1})	0.671	0.595
Range of *h*, *k*, *l*	h = −11 → 7 k = −16 → 16 l = −23 → 22	h = −29 → 29 k = −5 → 9 l = −26 → 22
Refinement		
Refinement on	F^2	F^2
$R[F^2 > 2\sigma(F^2)]$, $wR(F^2)$, *S*	0.018, 0.038, 1.04	0.055, 0.163, 0.99
No. of reflections	8234	3414
No. of parameters	374	223
No. of restraints	0	18
H-atom treatment	H-atom parameters constrained	H-atom parameters constrained
Weighting scheme	w = 1/[σ2(Fo2) + (0.0198P)2 + 0.8853P] where P = (Fo2 + 2Fc2)/3	*w = 1/[σ2(Fo2) + (0.1072P)2]* where P = (Fo2 + 2Fc2)/3
$(\Delta/\sigma)_{max}$	< 0.001	< 0.001
$\Delta\rho_{max}$, $\Delta\rho_{min}$ (e Å^{-3})	0.62, −0.54	2.14, −2.78

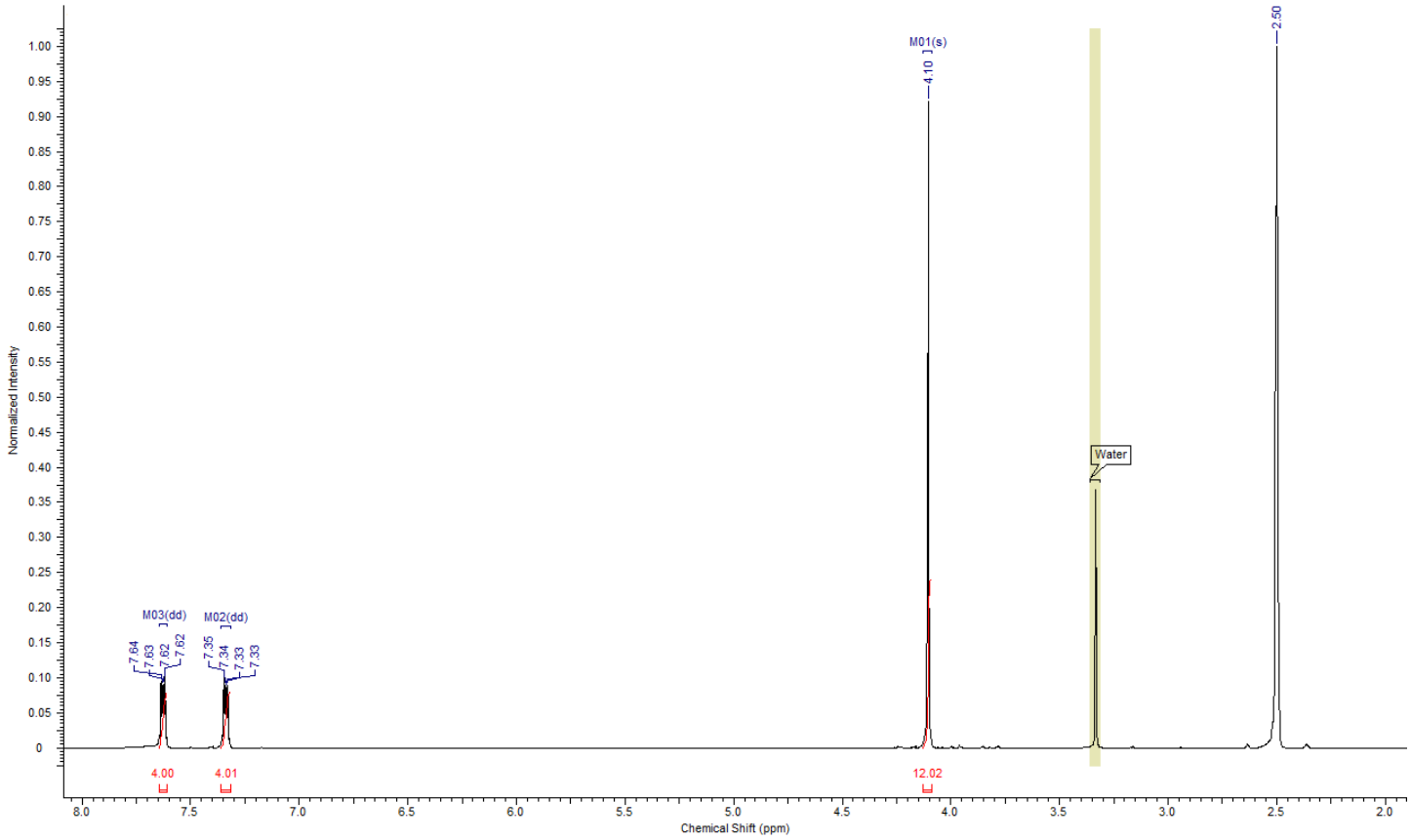

Fig. S 1: ^{1}H-NMR spectrum (500 MHz, DMSO-d_6) of complex **2a**.

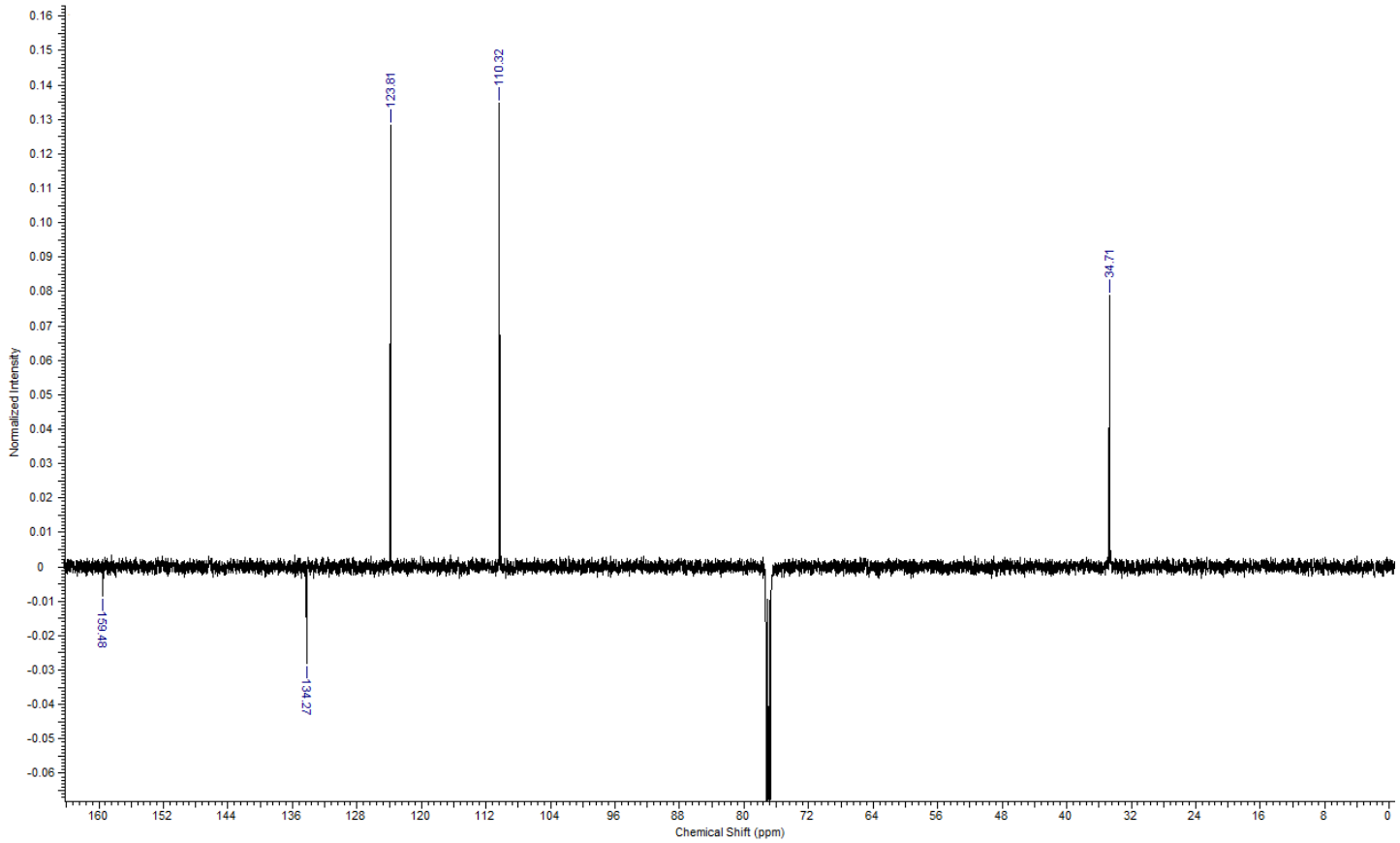

Fig. S 2: ^{13}C-NMR spectrum (126 MHz, $CDCl_3$) of complex **2a**.

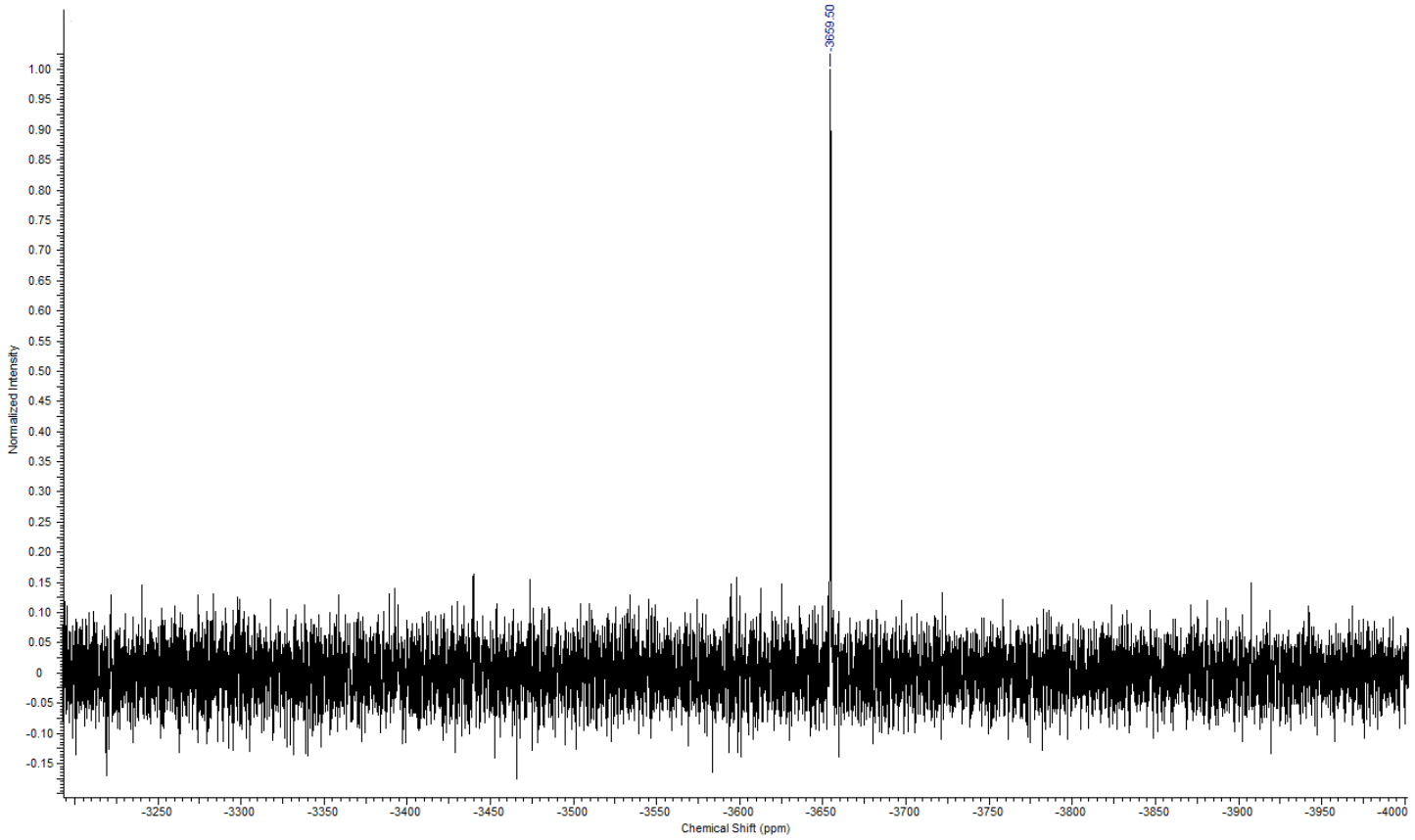

Fig. S 3: ^{195}Pt-NMR spectrum (108 MHz, $CDCl_3$) of complex **2a**.

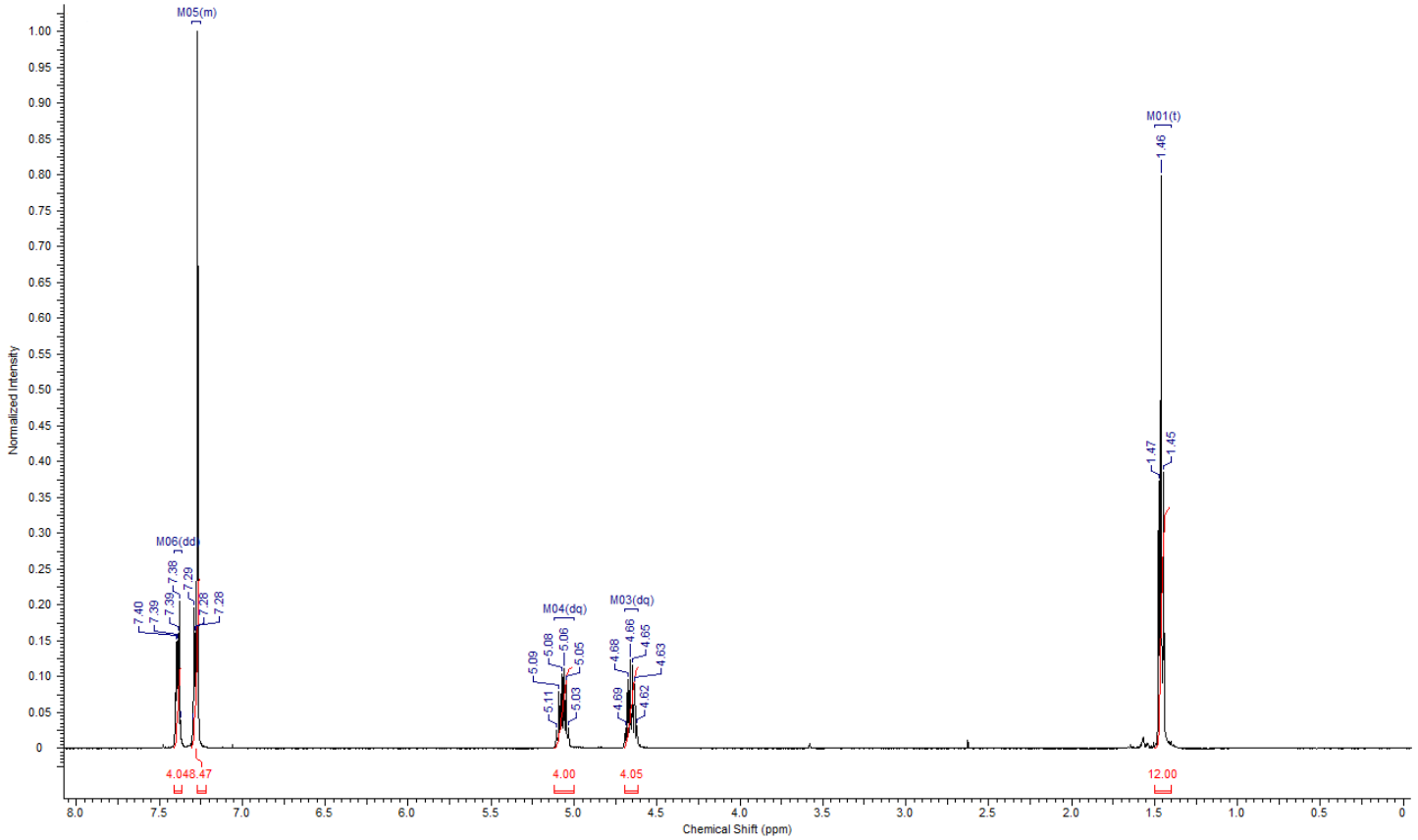

Fig. S 4: ^{1}H-NMR spectrum (500 MHz, $CDCl_3$) of complex **2b**.

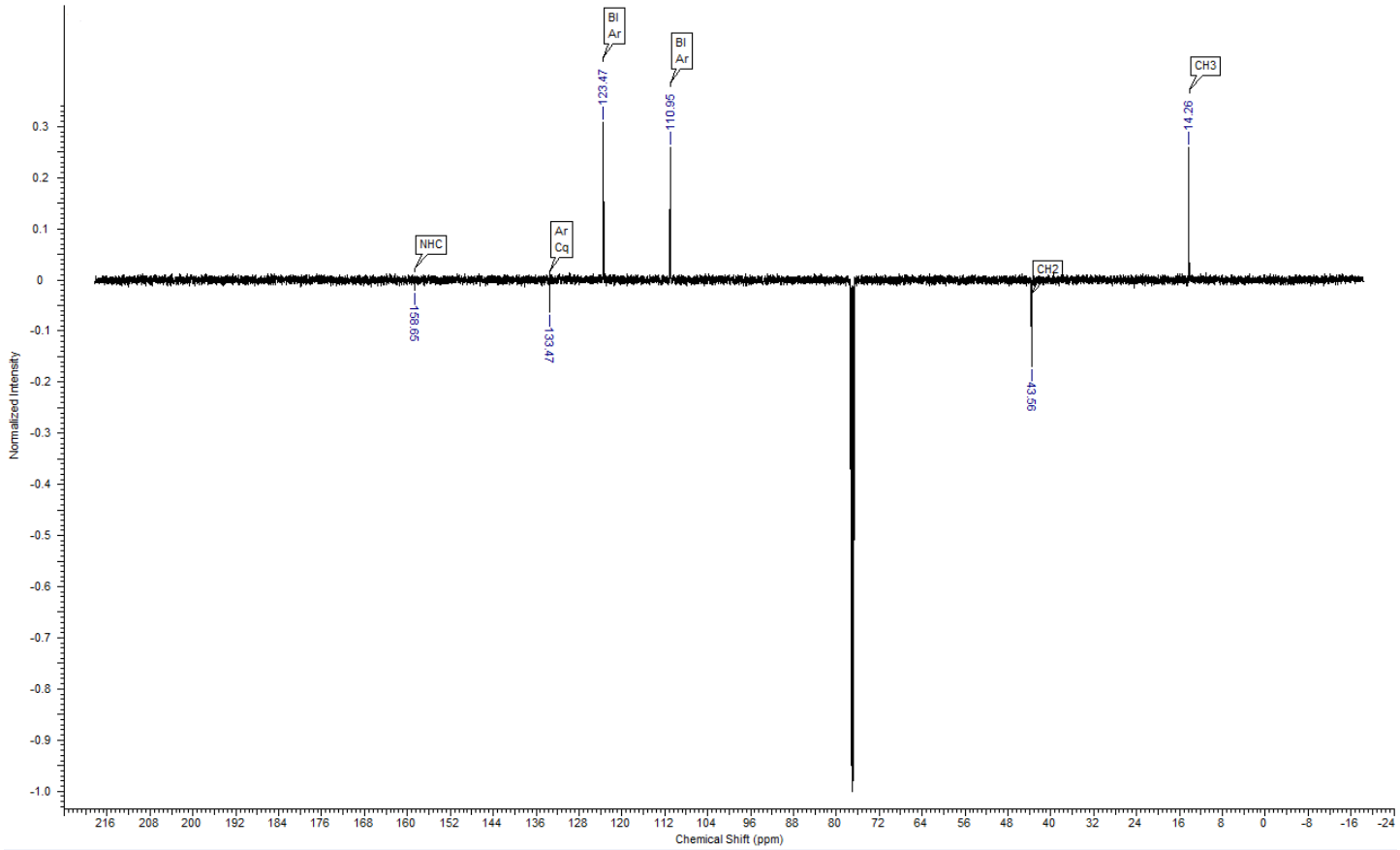

Fig. S 5: ^{13}C-NMR spectrum (126 MHz, $CDCl_3$) of complex **2b**.

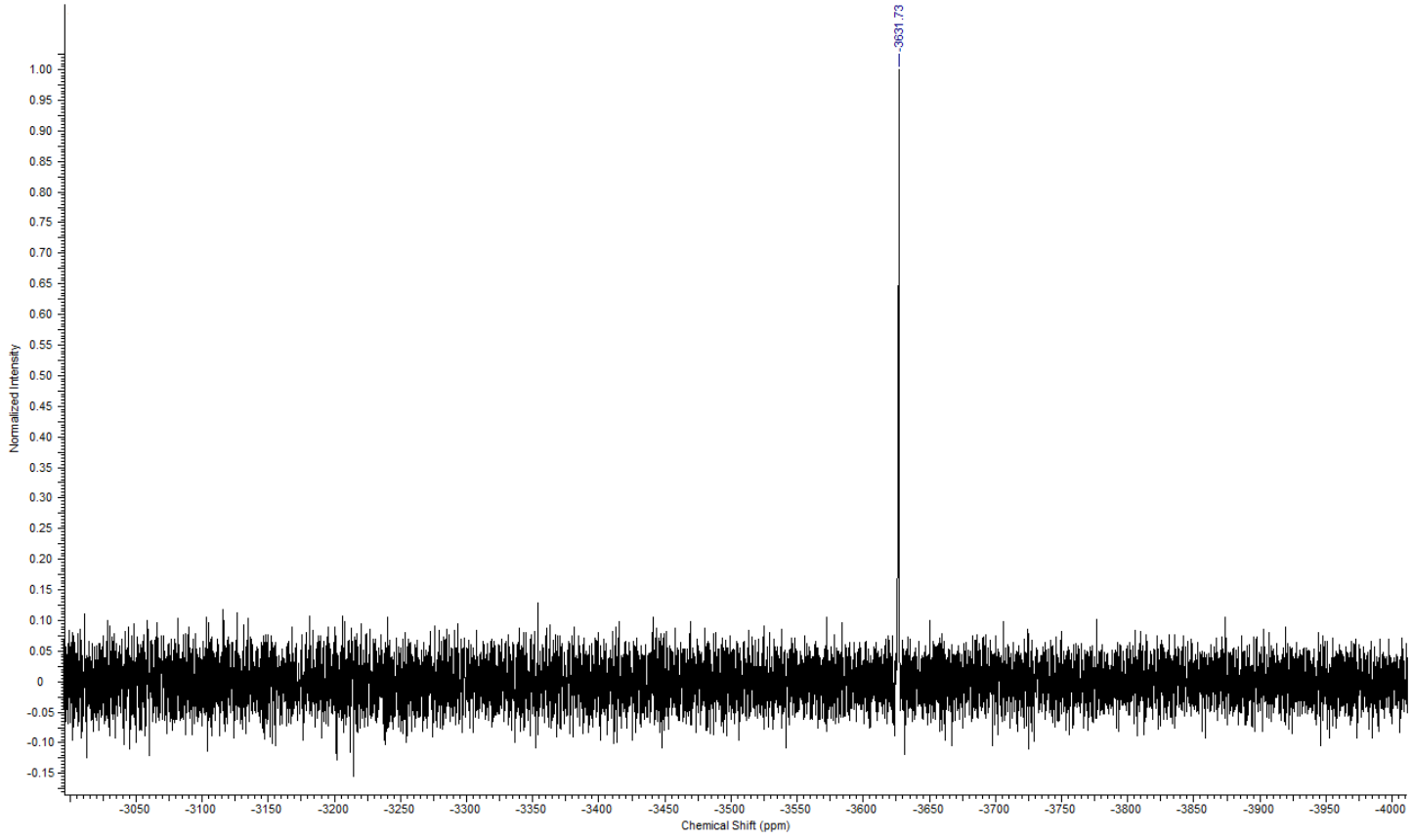

Fig. S 6: ^{195}Pt-NMR spectrum (108 MHz, $CDCl_3$) of complex **2b**.

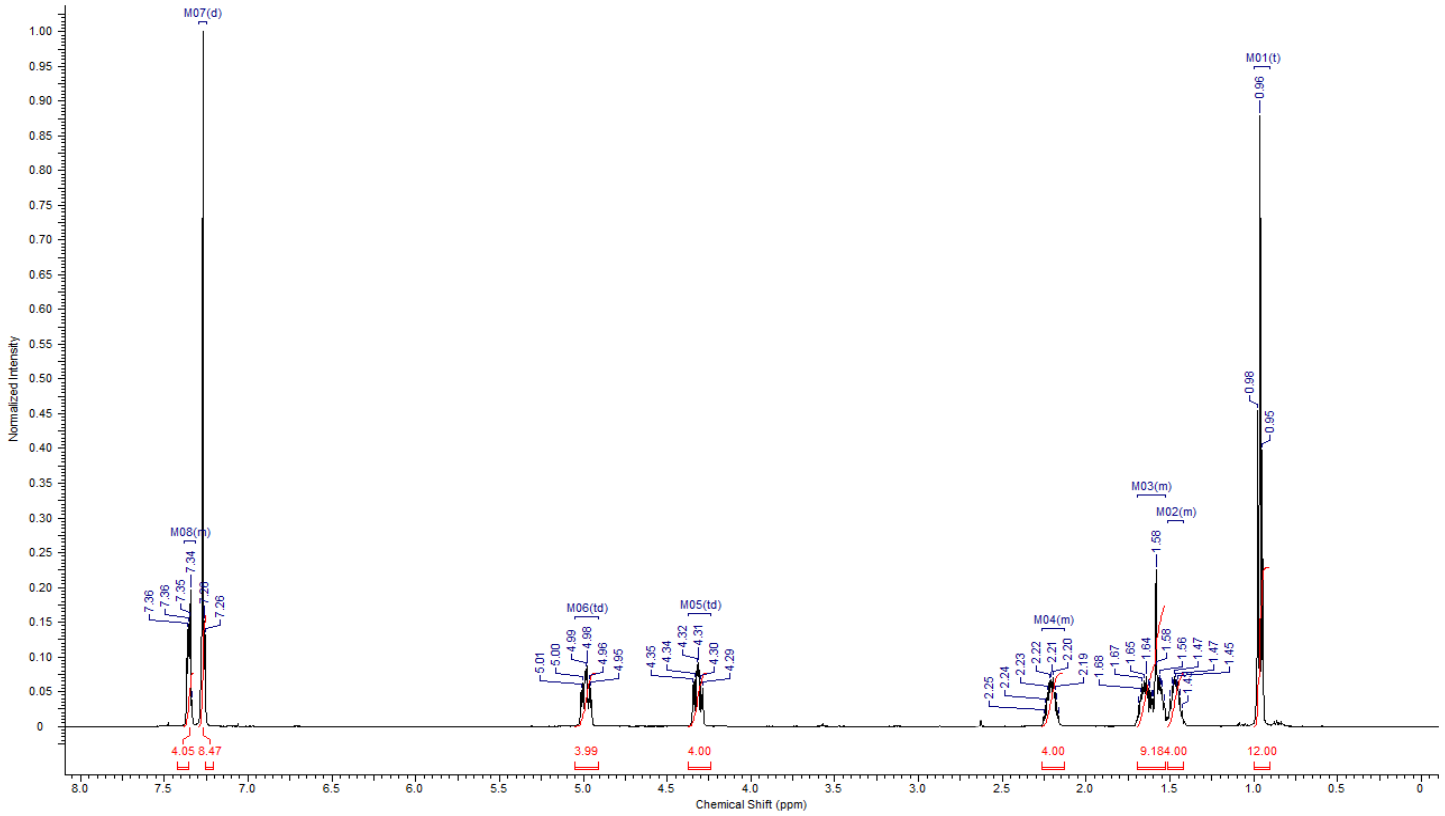

Fig. S 7: ^{1}H-NMR spectrum (500 MHz, $CDCl_3$) of complex **2c**.

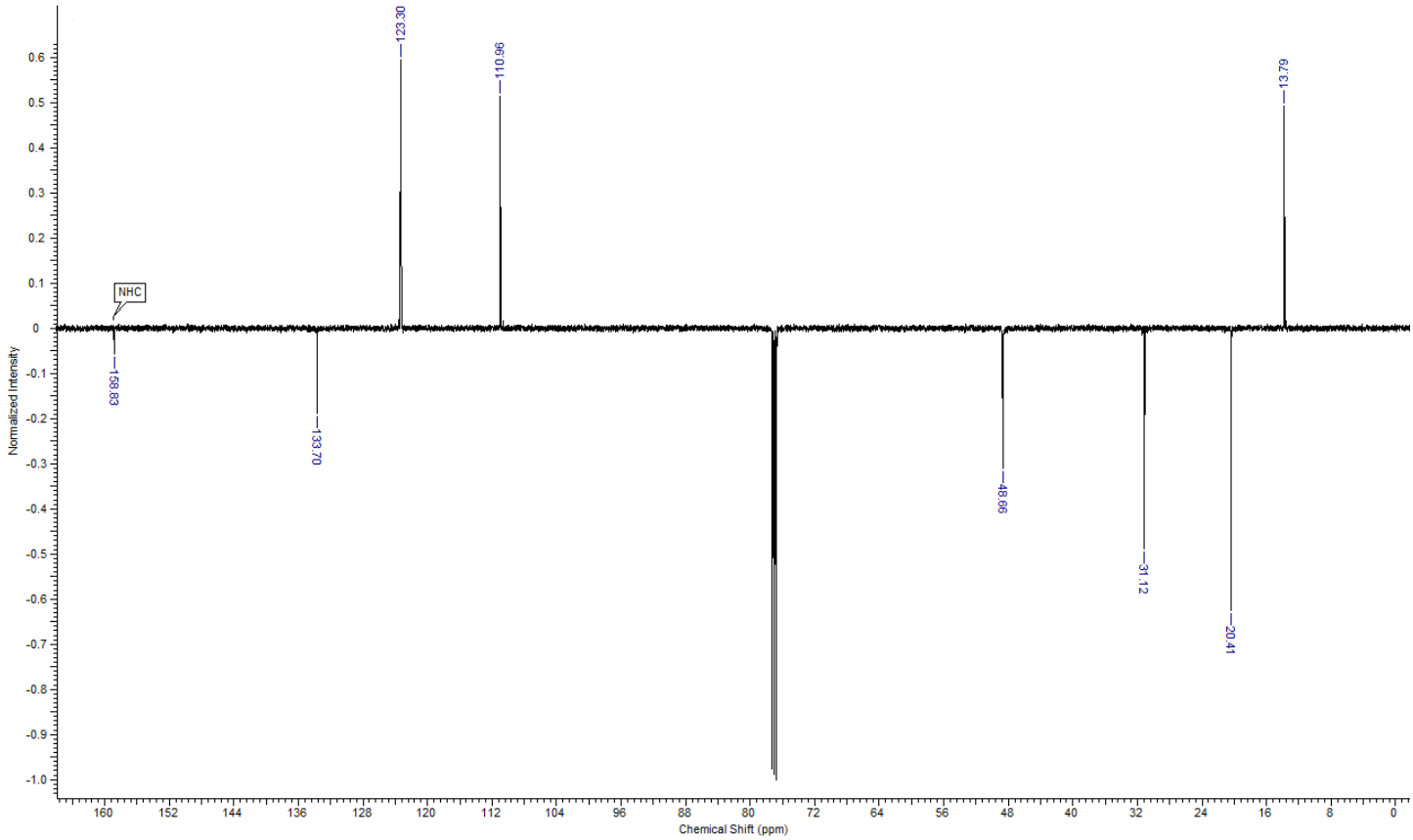

Fig. S 8: ^{13}C-NMR spectrum (126 MHz, $CDCl_3$) of complex **2c**.

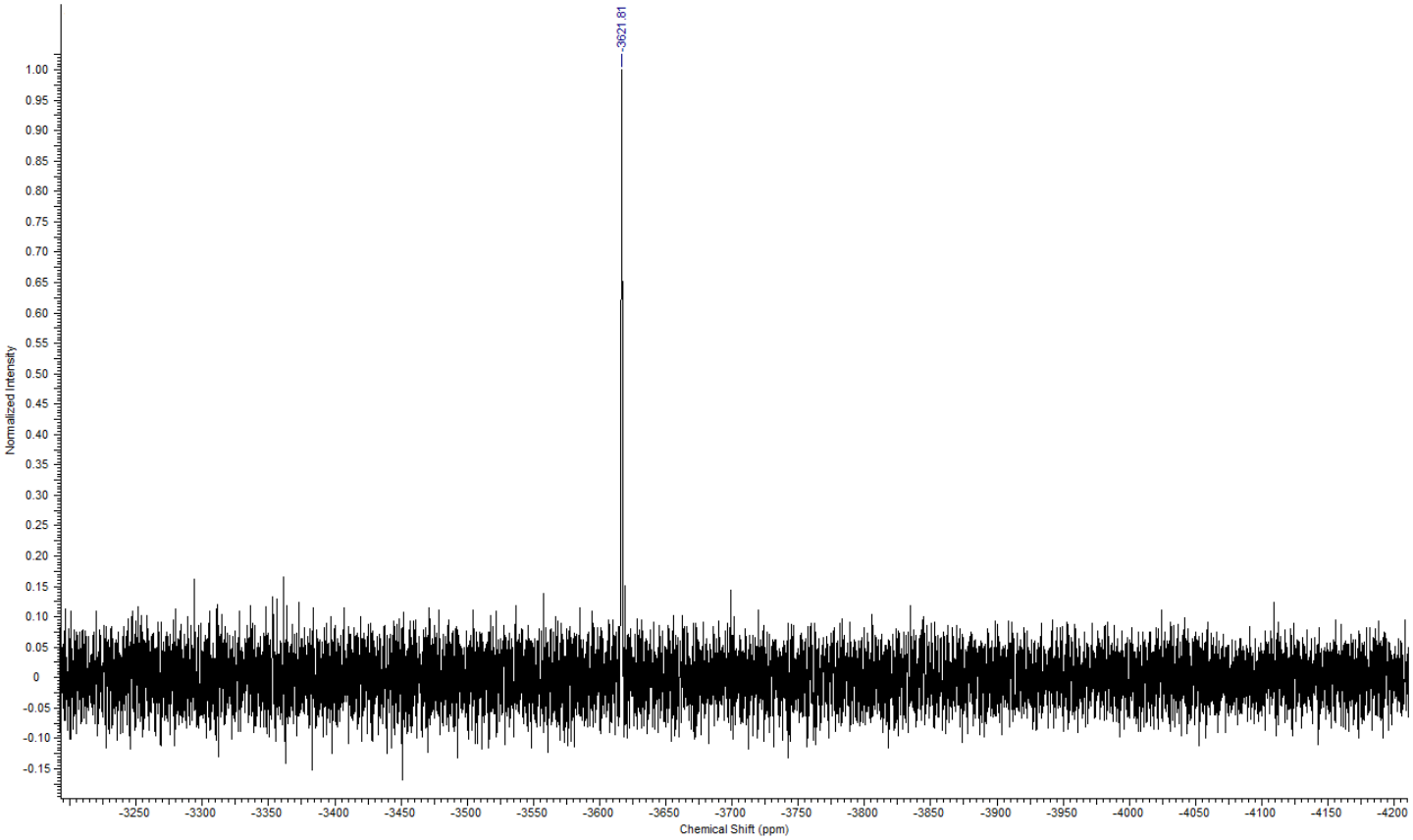

Fig. S 9: ^{195}Pt-NMR spectrum (108 MHz, $CDCl_3$) of complex **2c**.

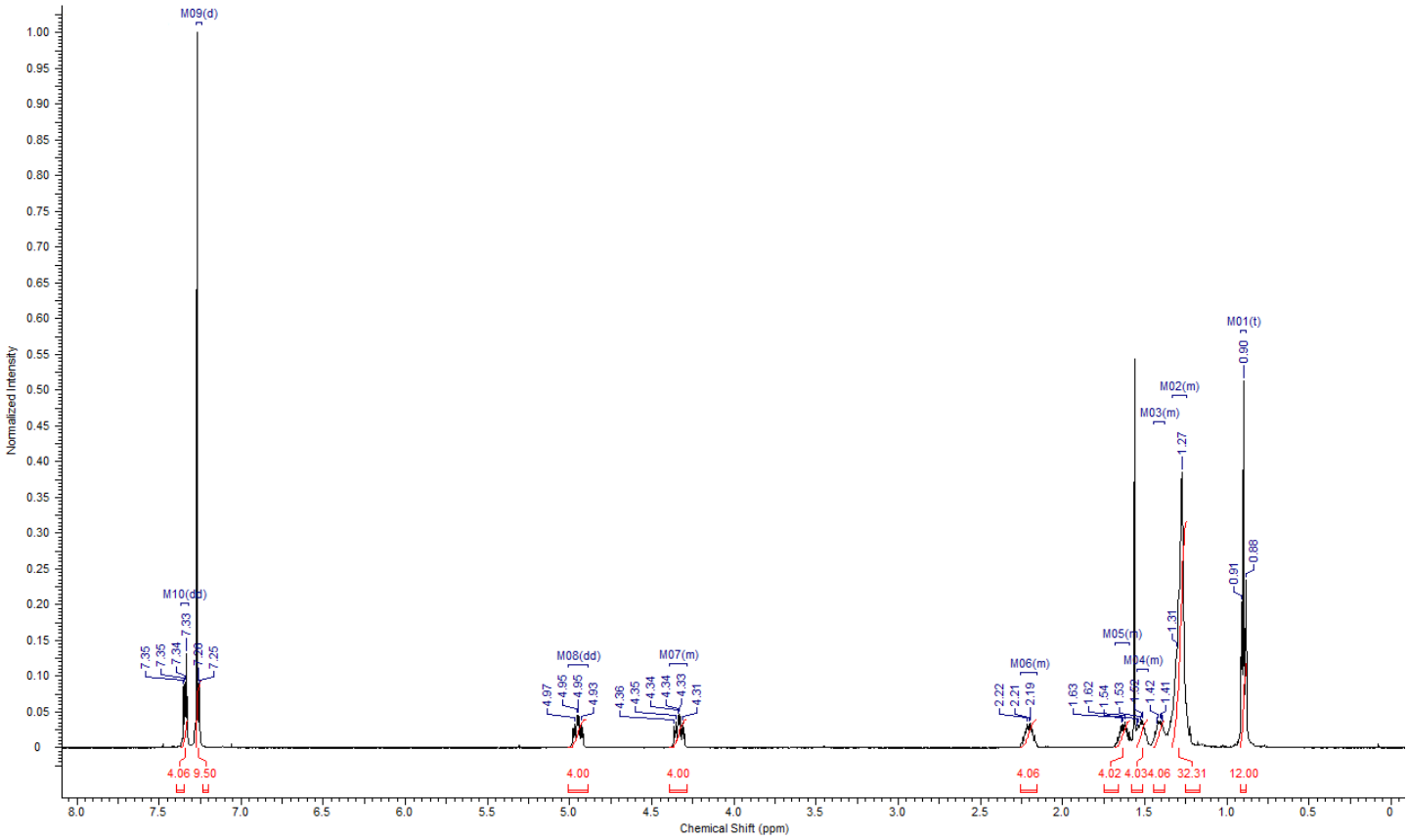

Fig. S 10: ^{1}H-NMR spectrum (500 MHz, $CDCl_3$) of complex **2d**.

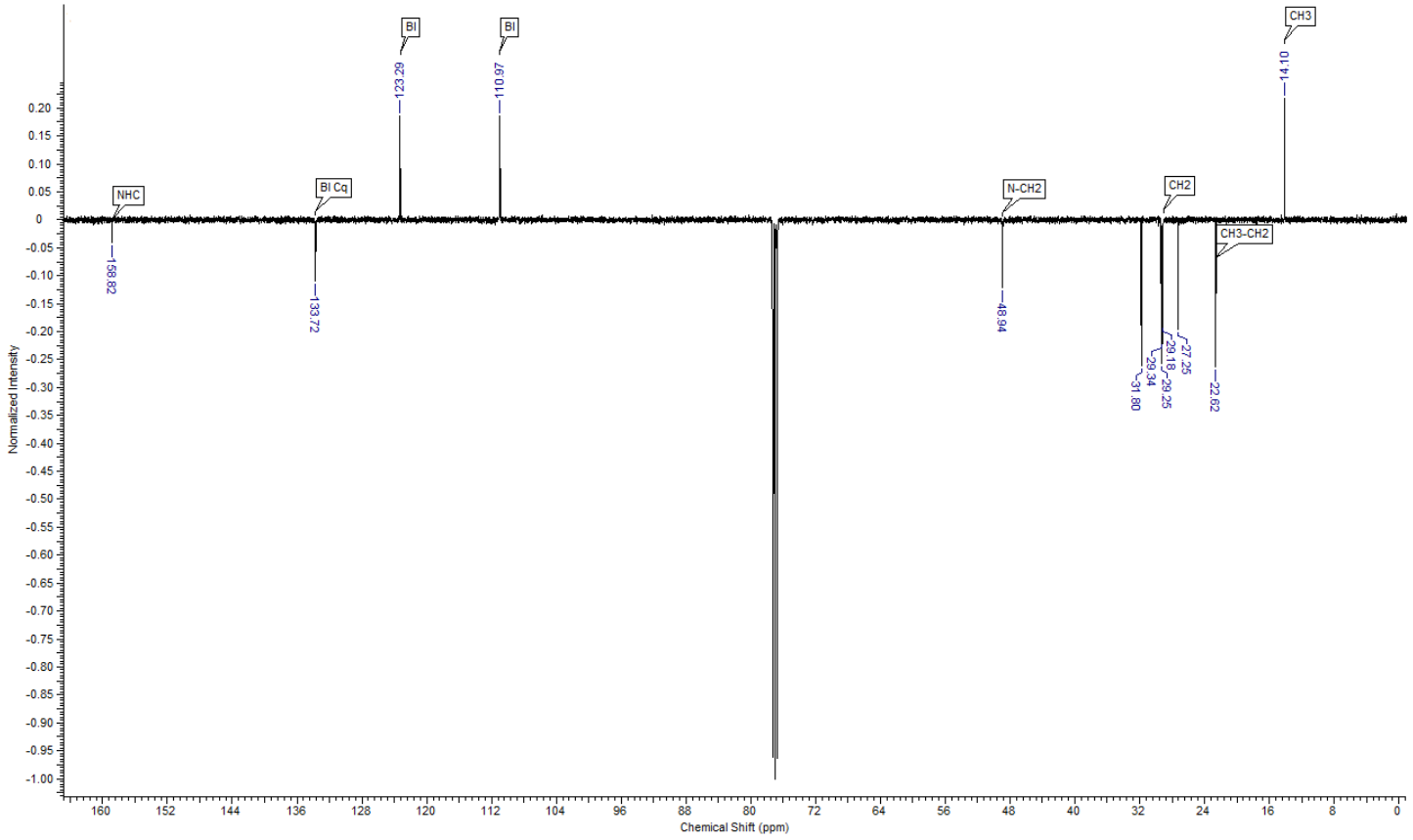

Fig. S 11: ^{13}C-NMR spectrum (126 MHz, $CDCl_3$) of complex **2d**.

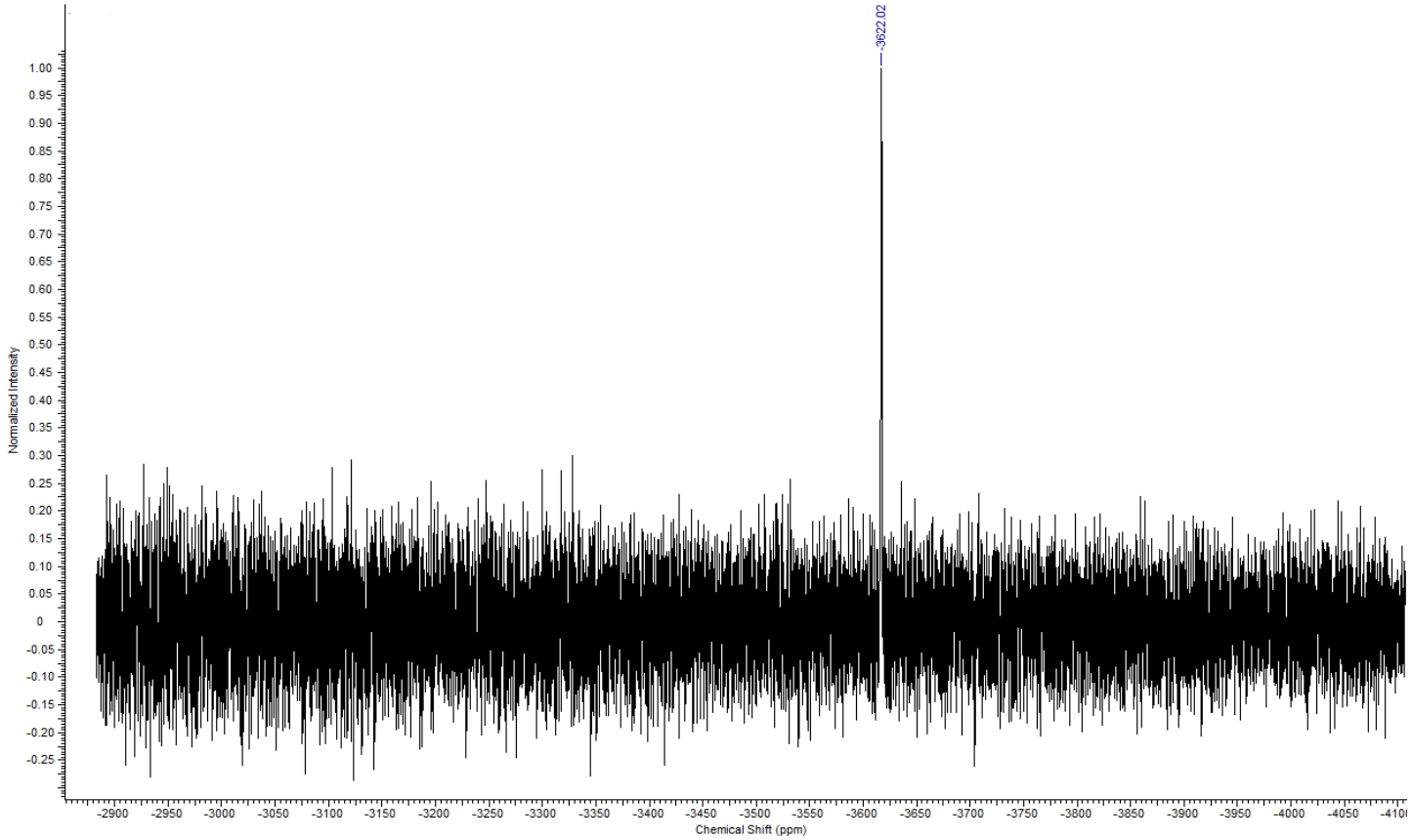

Fig. S 12: ^{195}Pt-NMR spectrum (108 MHz, $CDCl_3$) of complex **2d**.

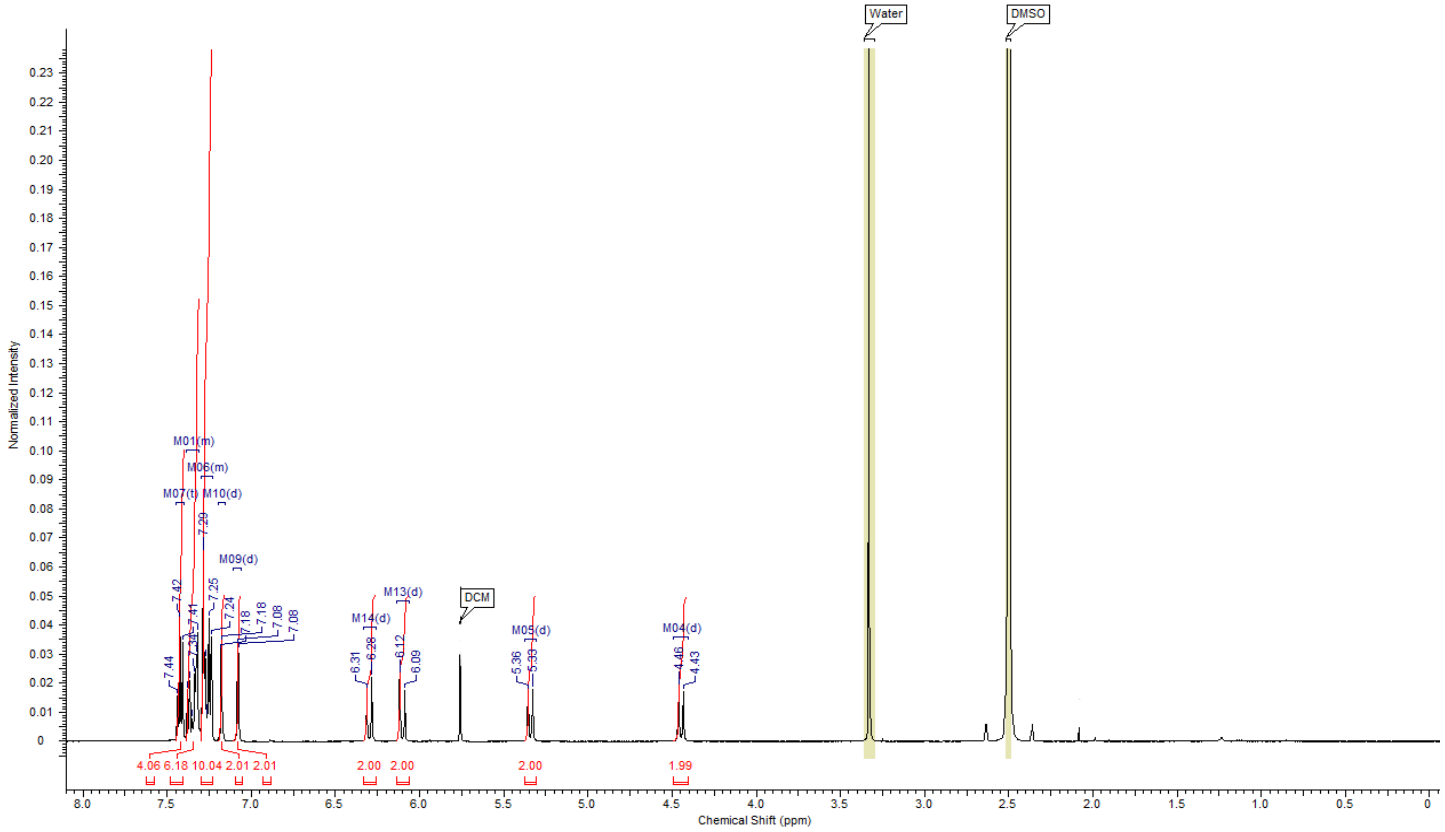

Fig. S 13: ^{1}H-NMR spectrum (500 MHz, DMSO-d_6) of complex **3**.

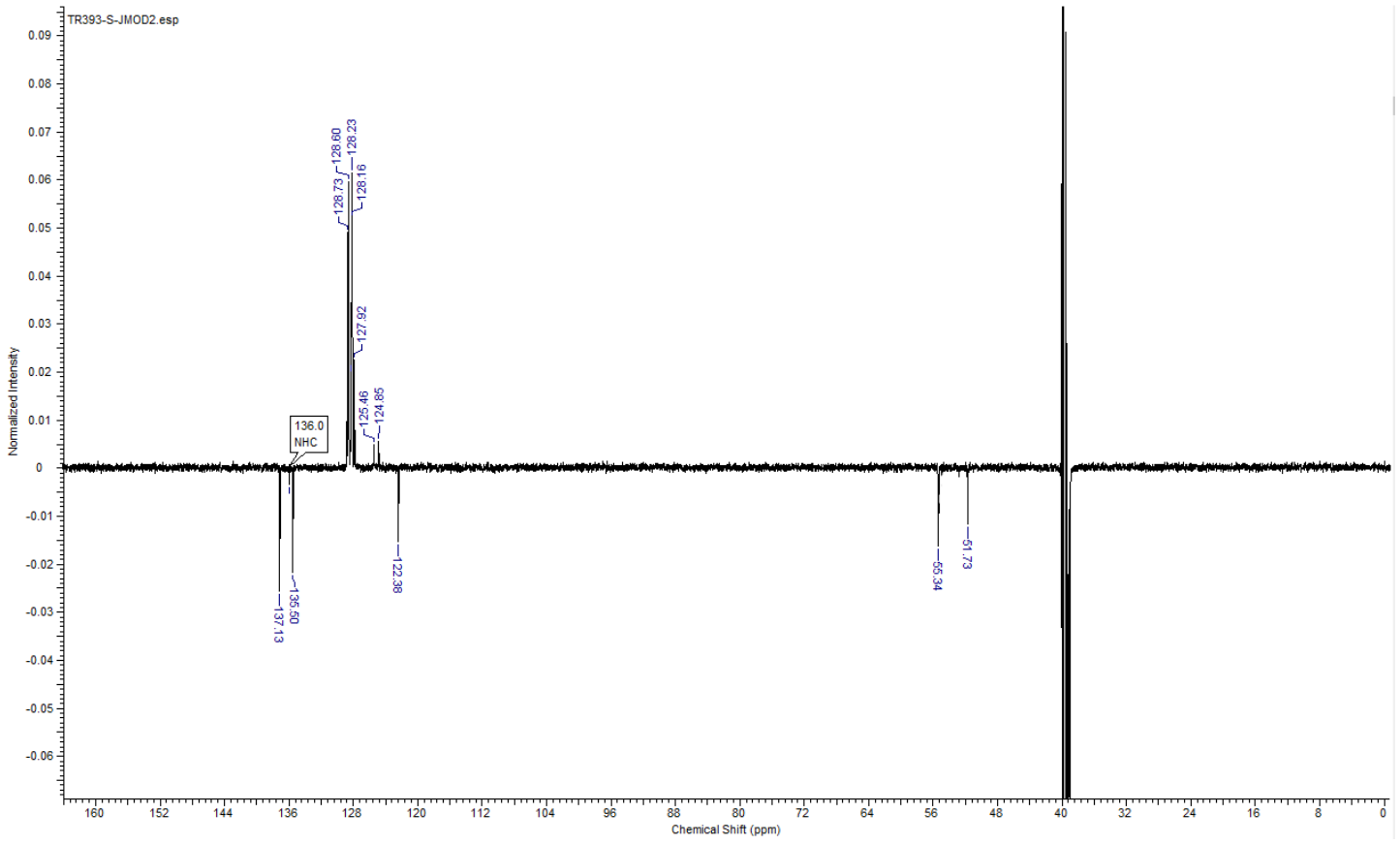

Fig. S 14: ^{13}C-NMR spectrum (126 MHz, DMSO-d_6) of complex **3**.

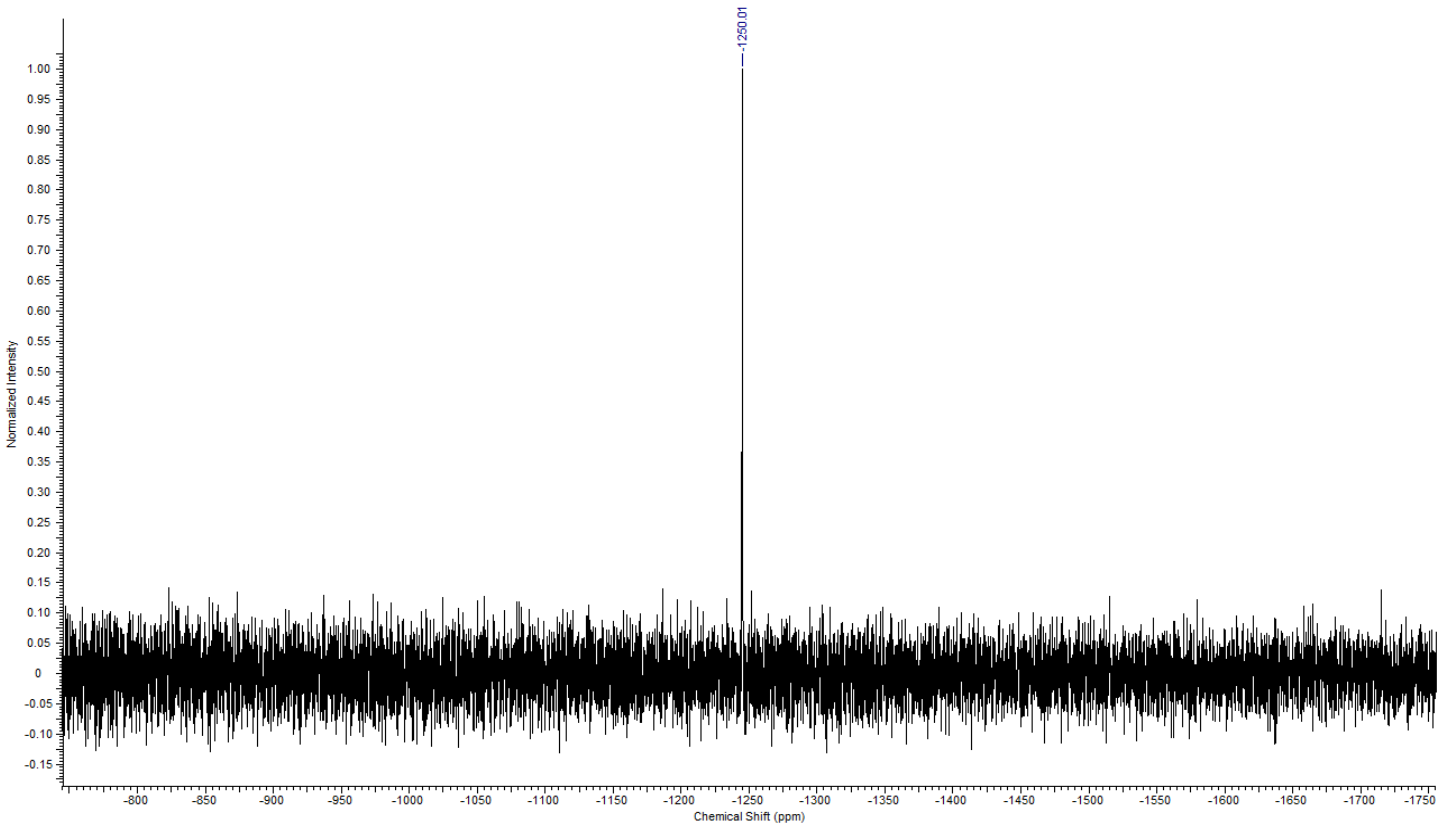

Fig. S 15: ^{195}Pt-NMR spectrum (108 MHz, DMSO-d_6) of complex **3**.

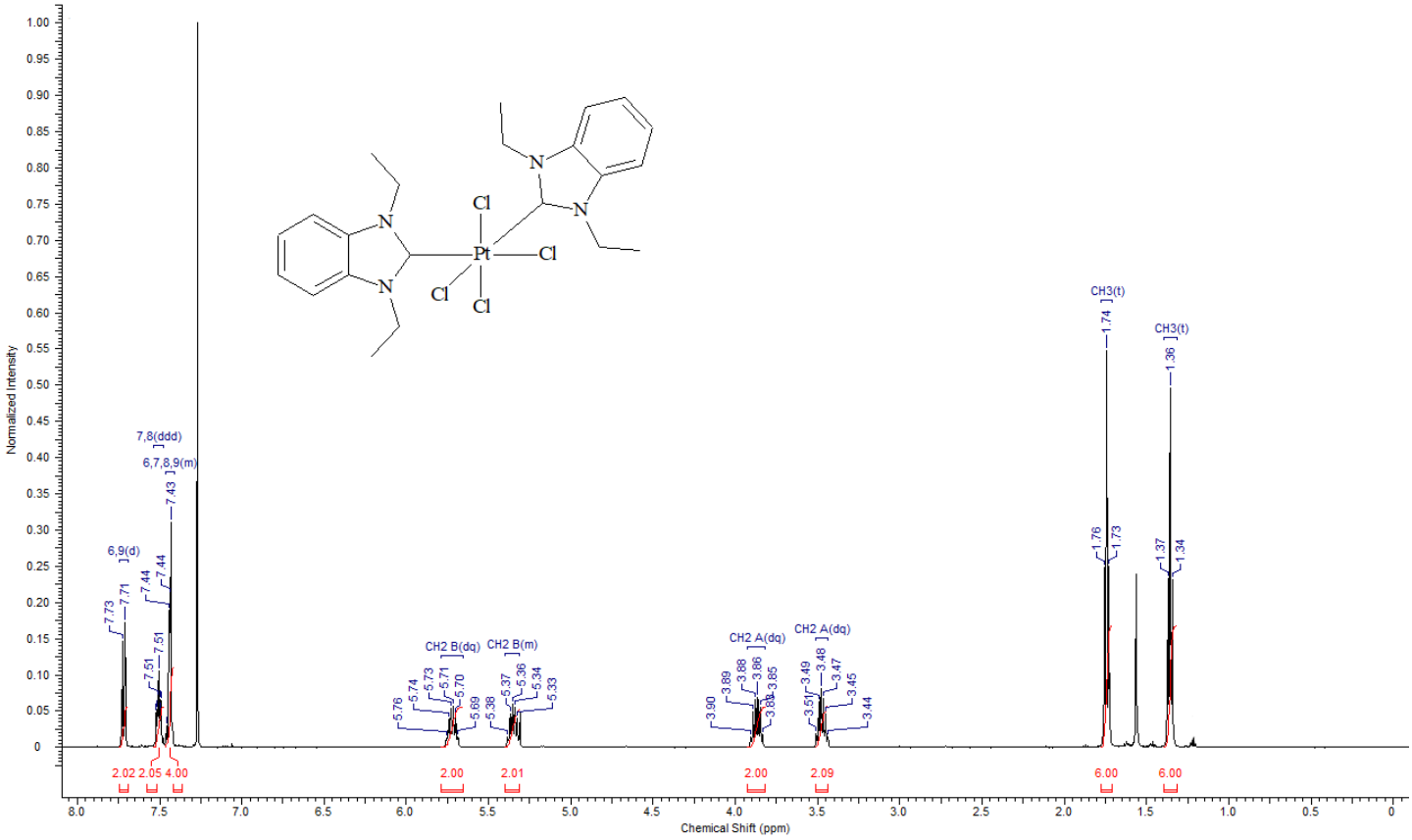

Fig. S 16: ^{1}H-NMR spectrum (500 MHz, $CDCl_3$) of complex **4b**.

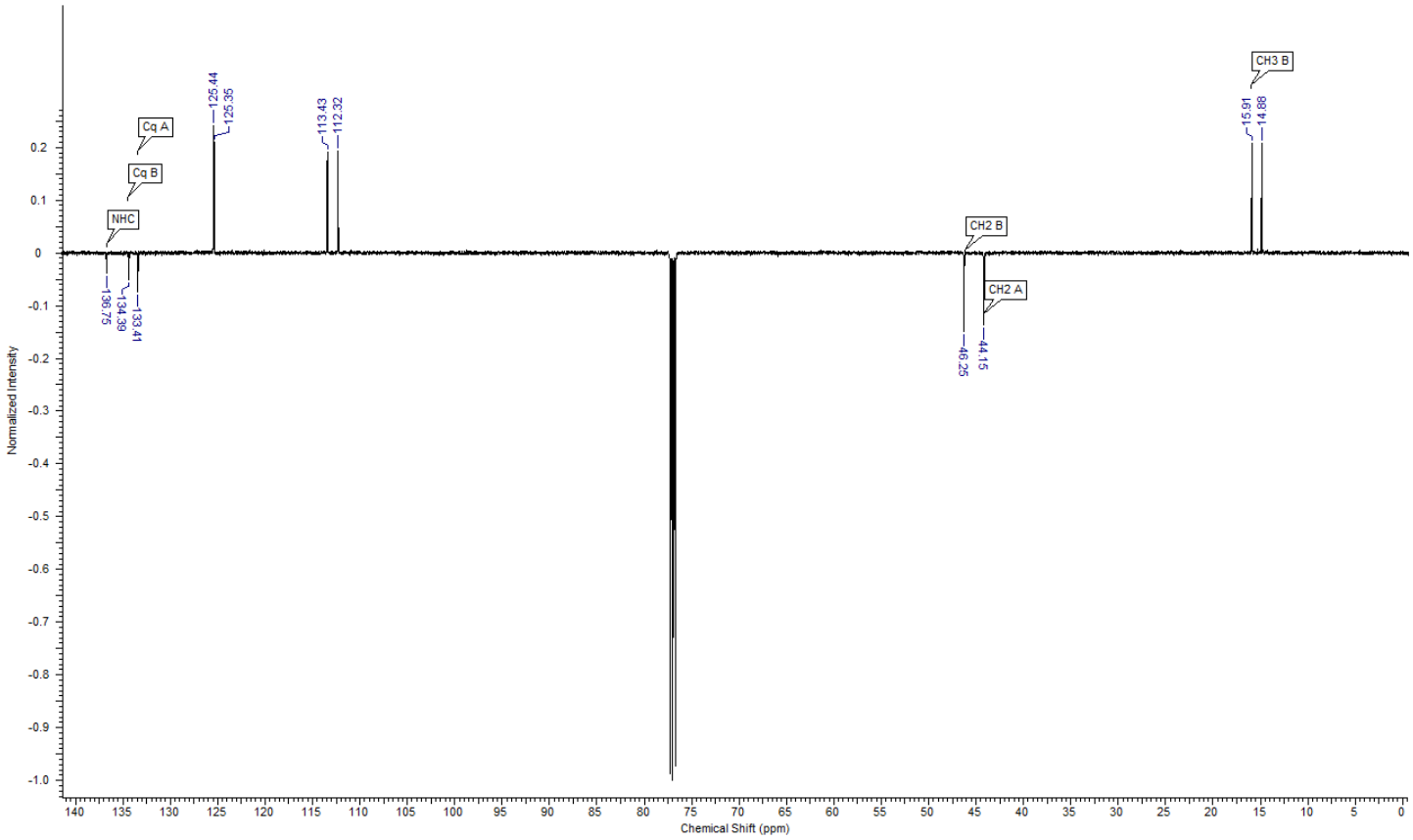

Fig. S 17: ^{13}C-NMR spectrum (126 MHz, $CDCl_3$) of complex **4b**.

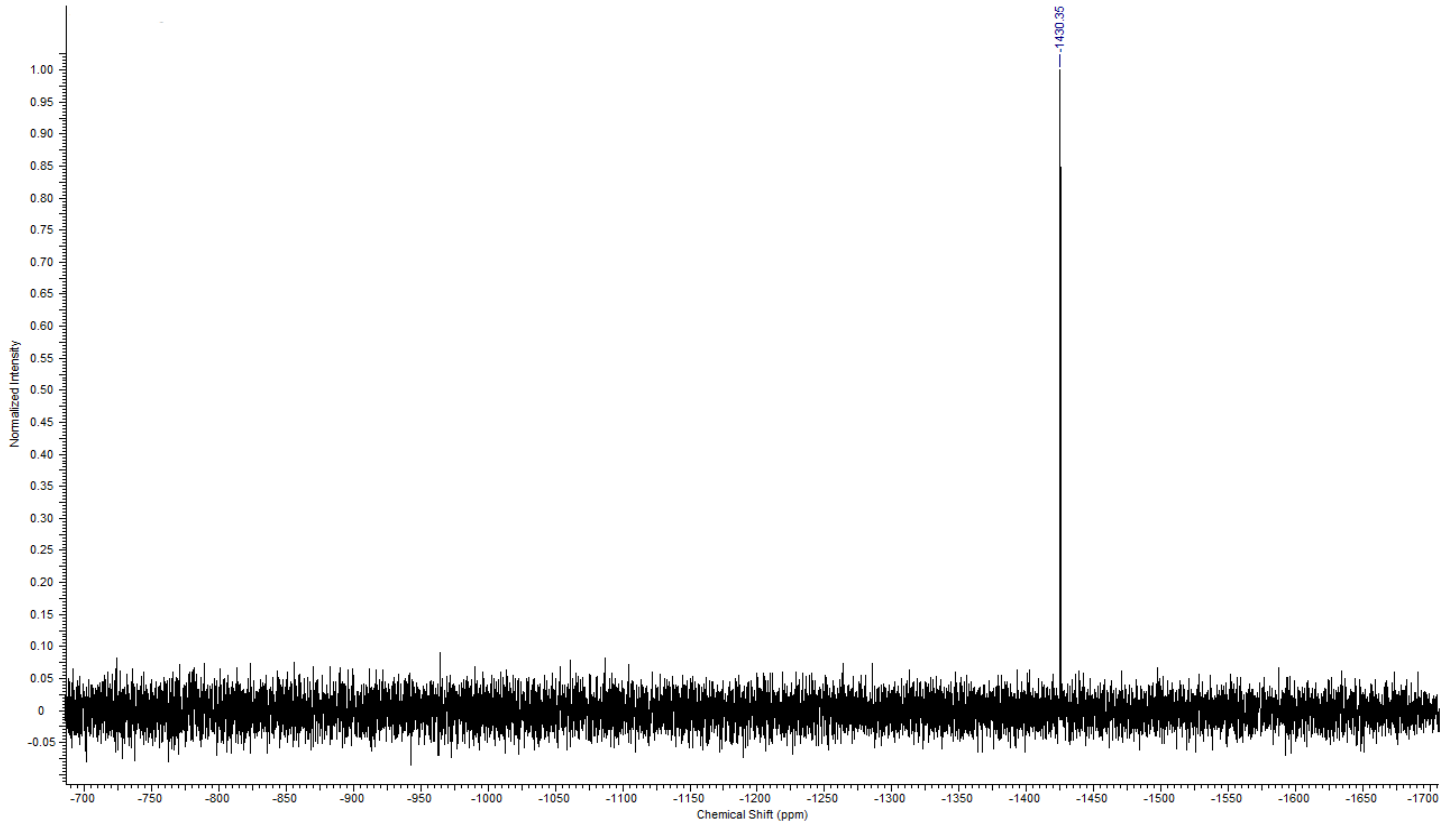

Fig. S 18: ^{195}Pt-NMR spectrum (108 MHz, $CDCl_3$) of complex **4b**.

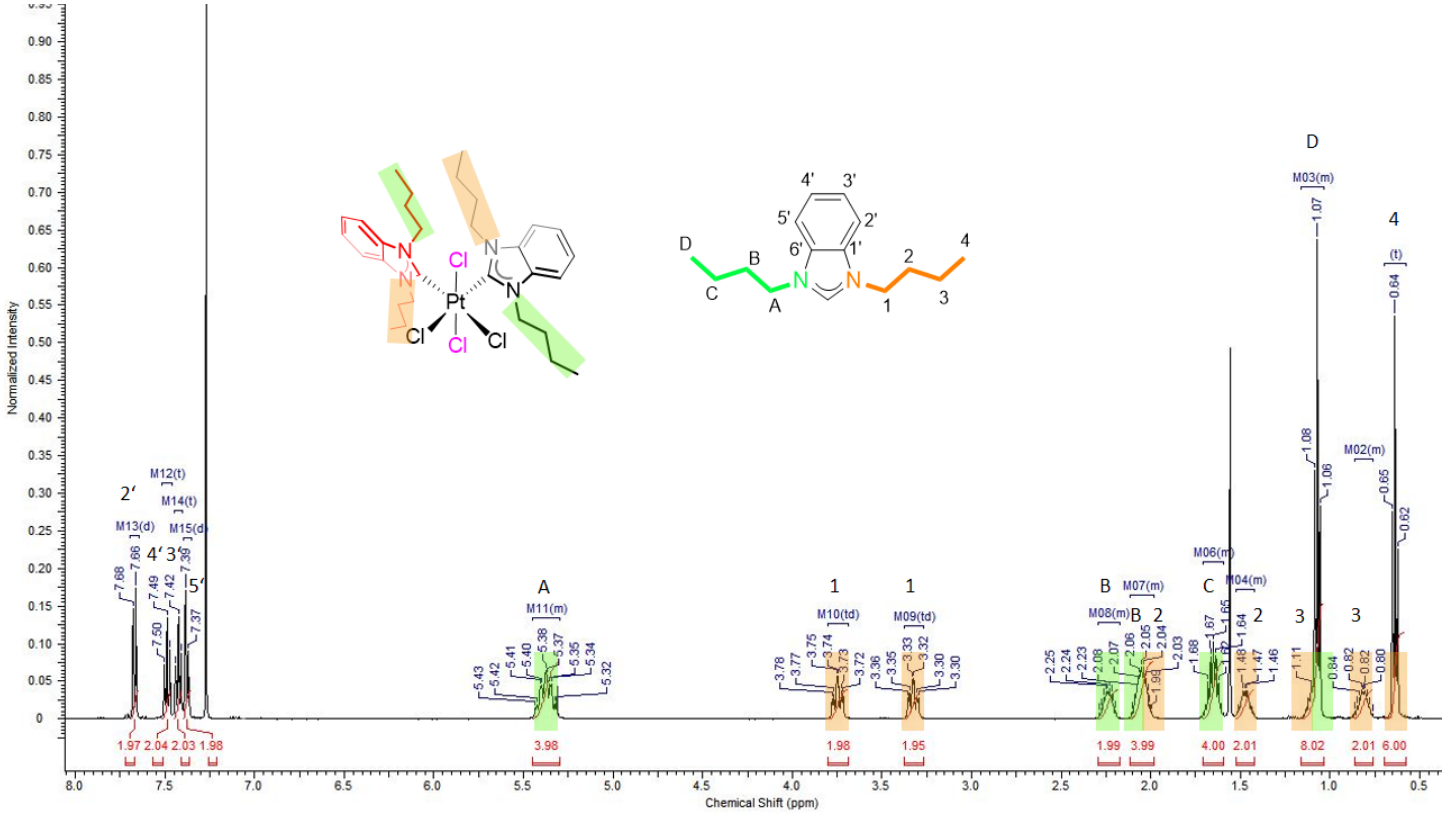

Fig. S 19: ^{1}H-NMR spectrum (500 MHz, $CDCl_3$) of complex **4c**.

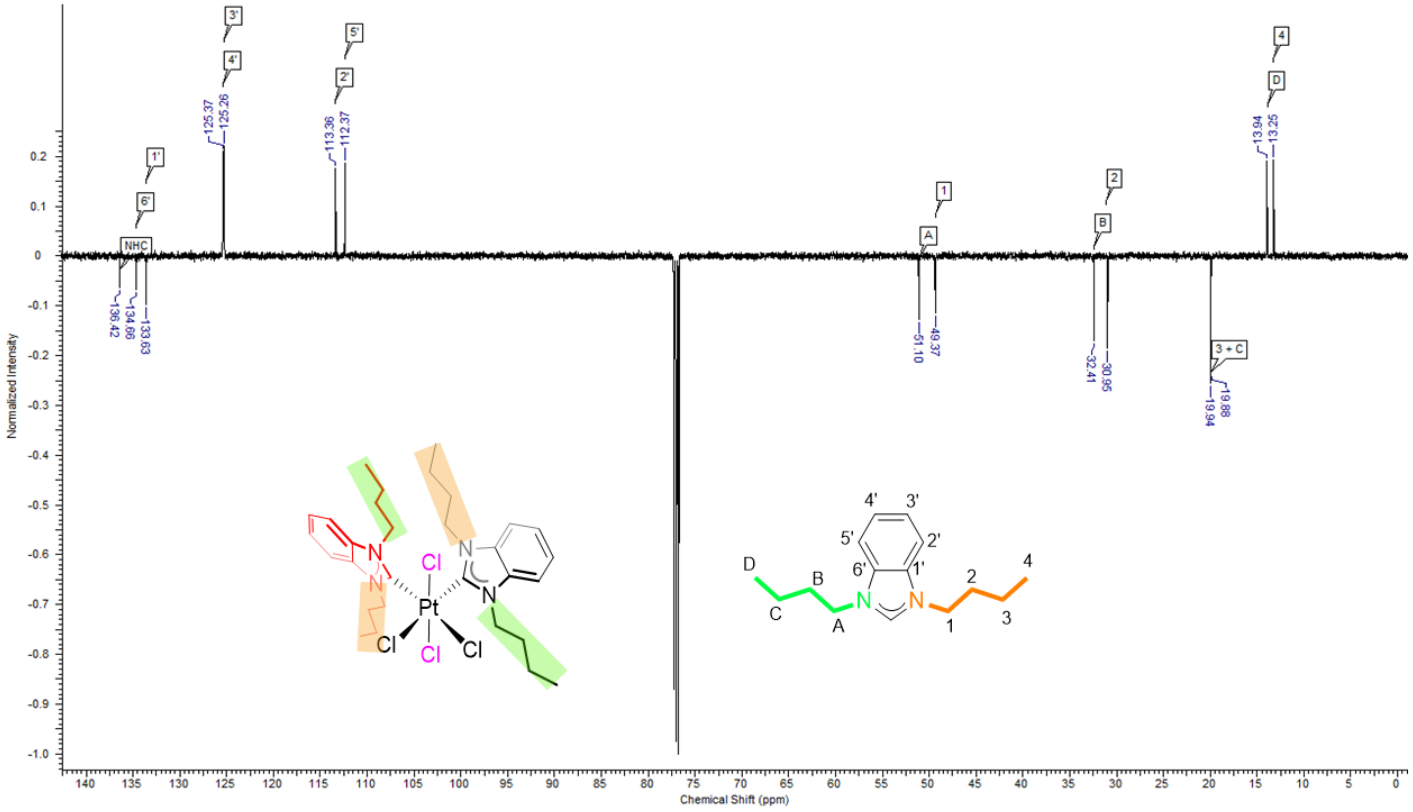

Fig. S 20: ^{13}C-NMR spectrum (126 MHz, $CDCl_3$) of complex **4c**.

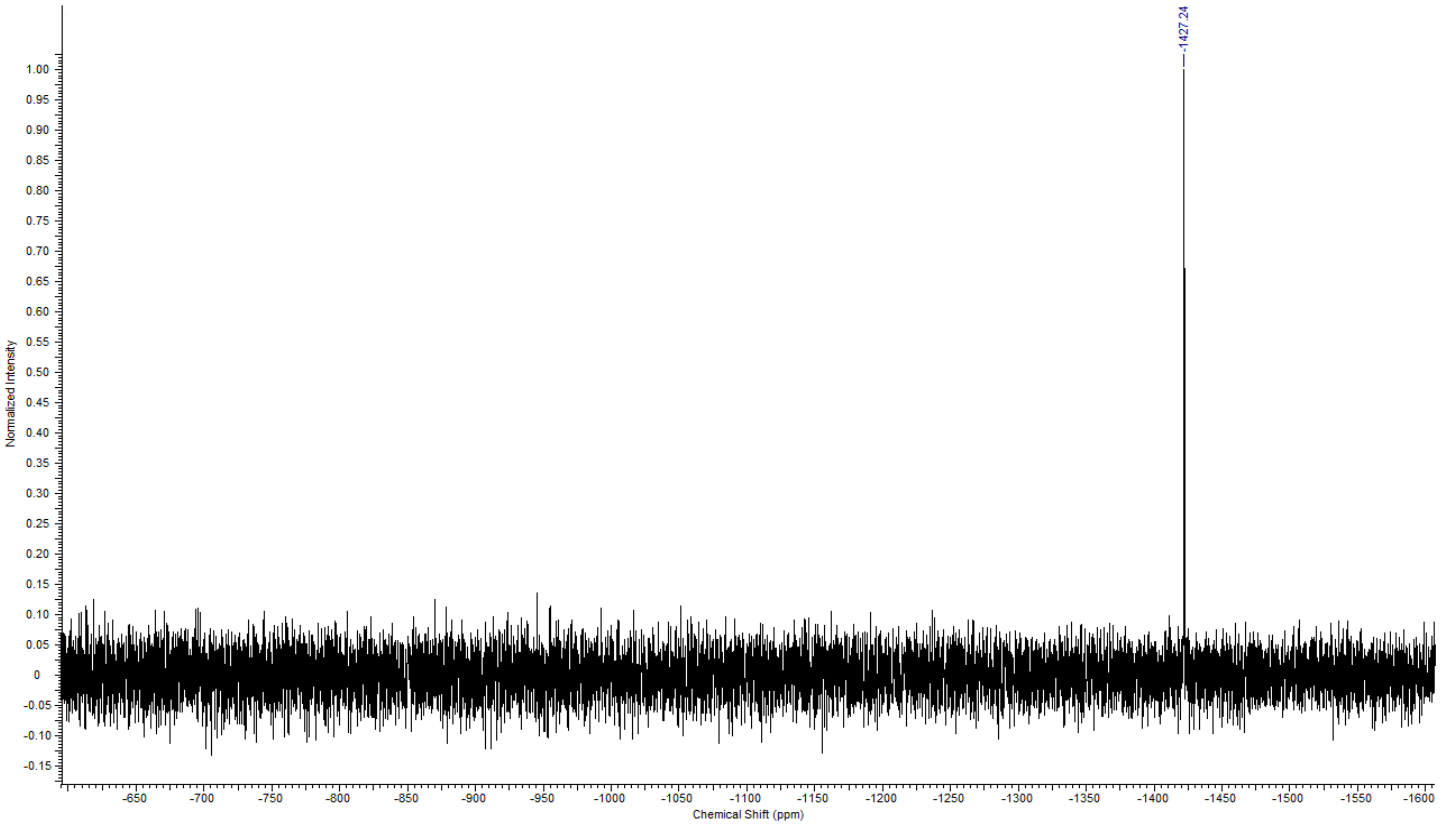

Fig. S 21: ^{195}Pt-NMR spectrum (108 MHz, $CDCl_3$) of complex **4c**.

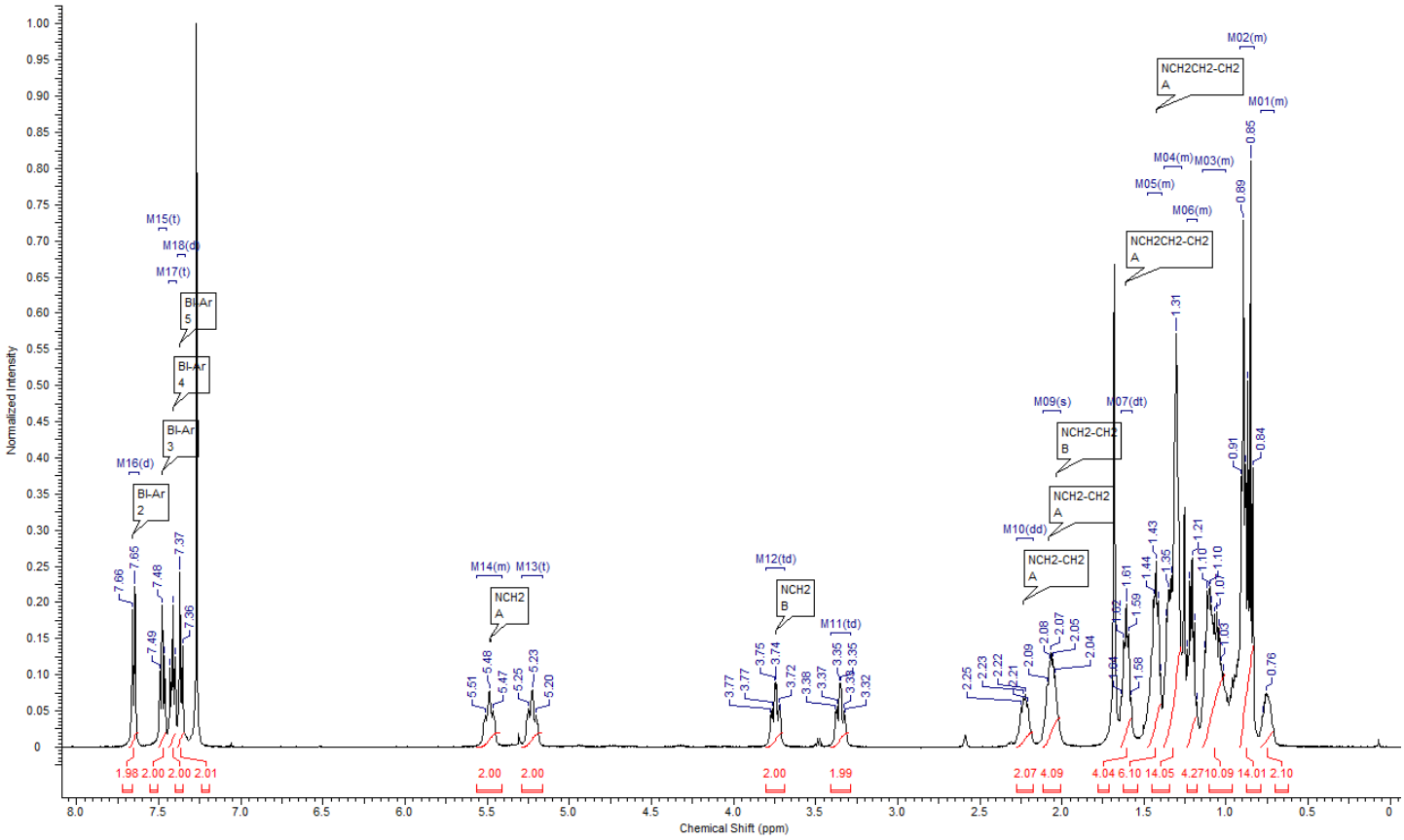

Fig. S 22: ^{1}H-NMR spectrum (500 MHz, $CDCl_3$) of complex **4d**.

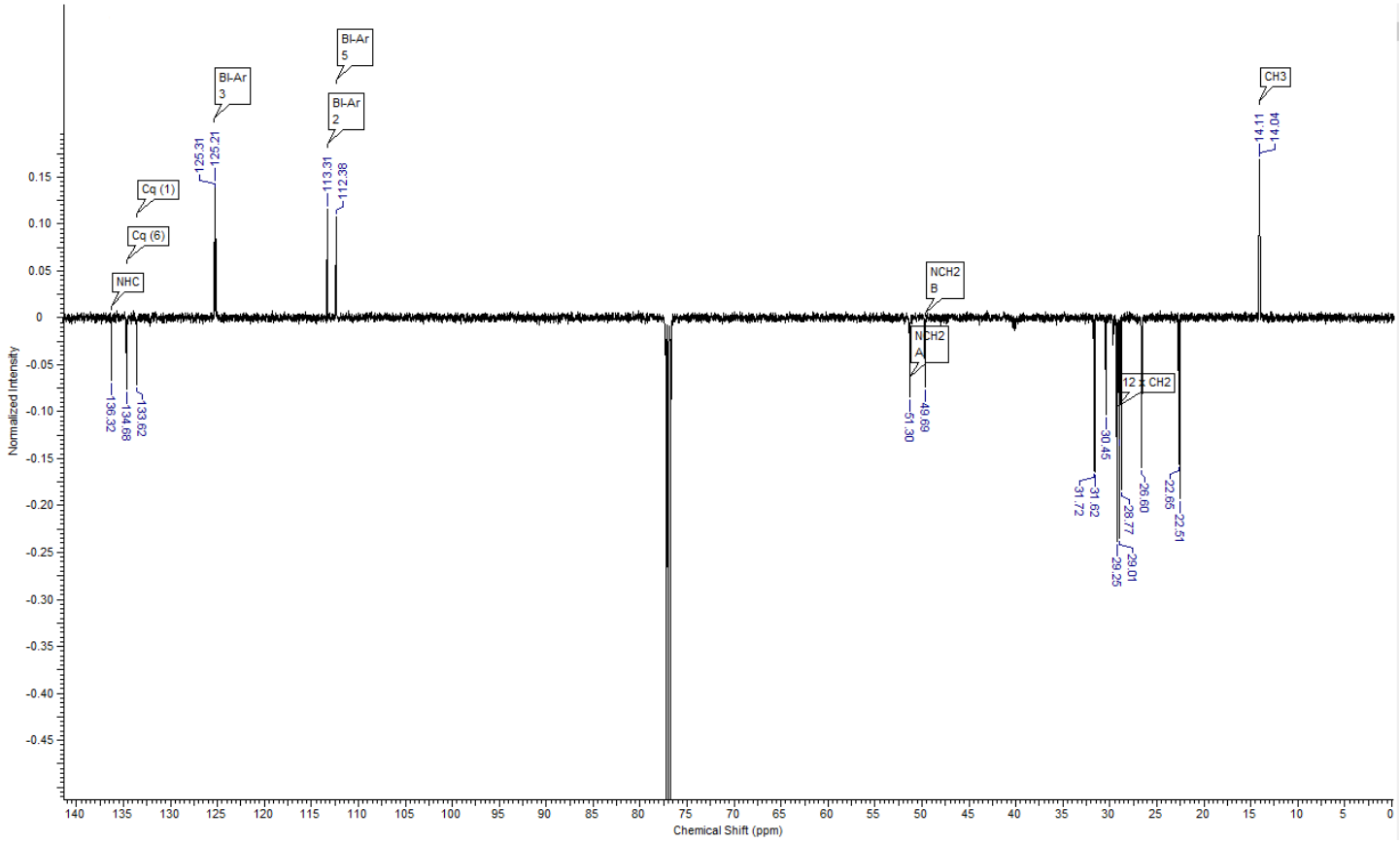

Fig. S 23: ^{13}C-NMR spectrum (126 MHz, $CDCl_3$) of complex **4d**.

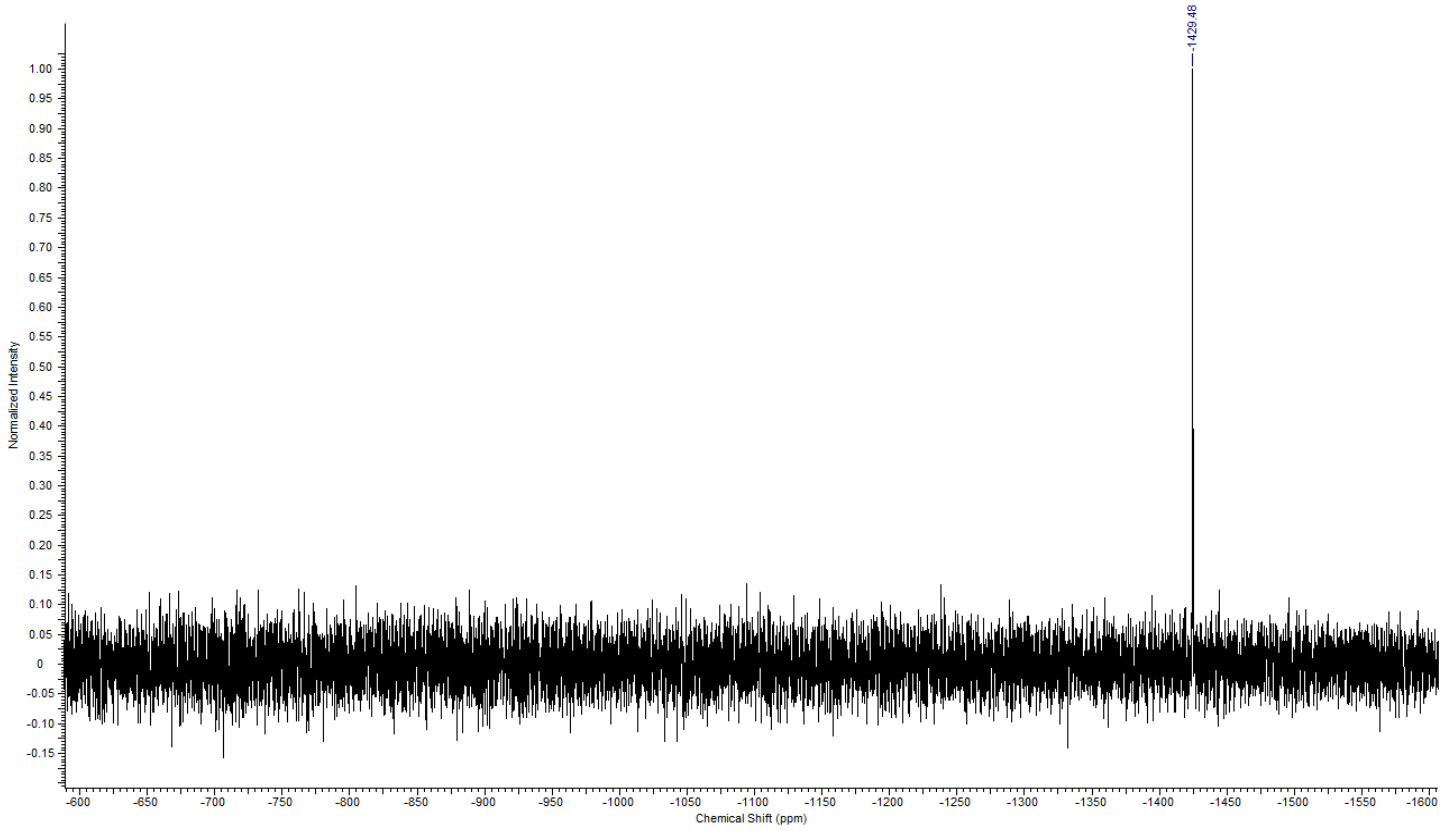

Fig. S 24: ^{195}Pt-NMR spectrum (108 MHz, $CDCl_3$) of complex **4d**.

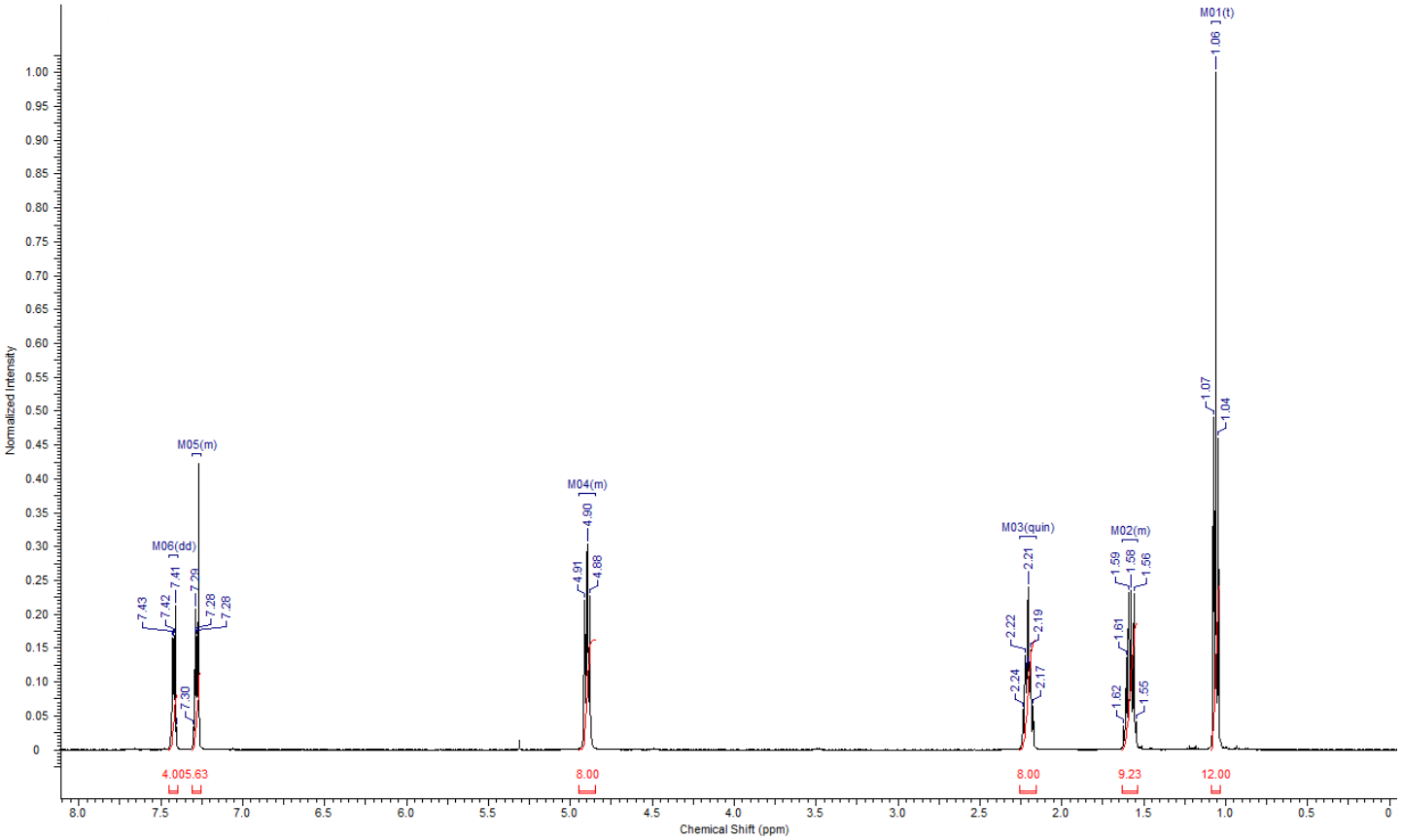

Fig. S 25: ^{1}H-NMR spectrum (500 MHz, $CDCl_3$) of complex ***trans*-2c**.

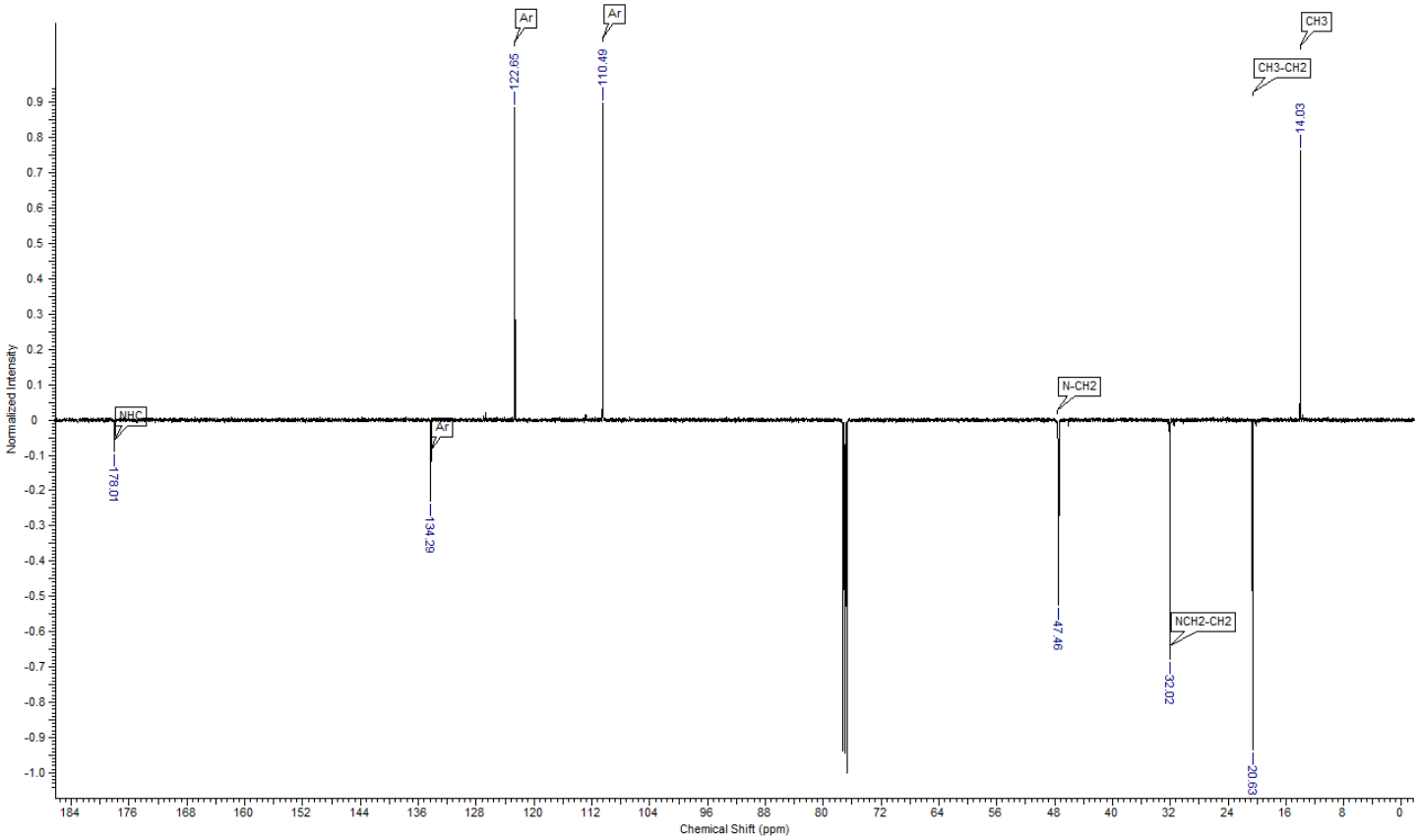

Fig. S 26: ^{13}C-NMR spectrum (126 MHz, $CDCl_3$) of complex ***trans*-2c**.

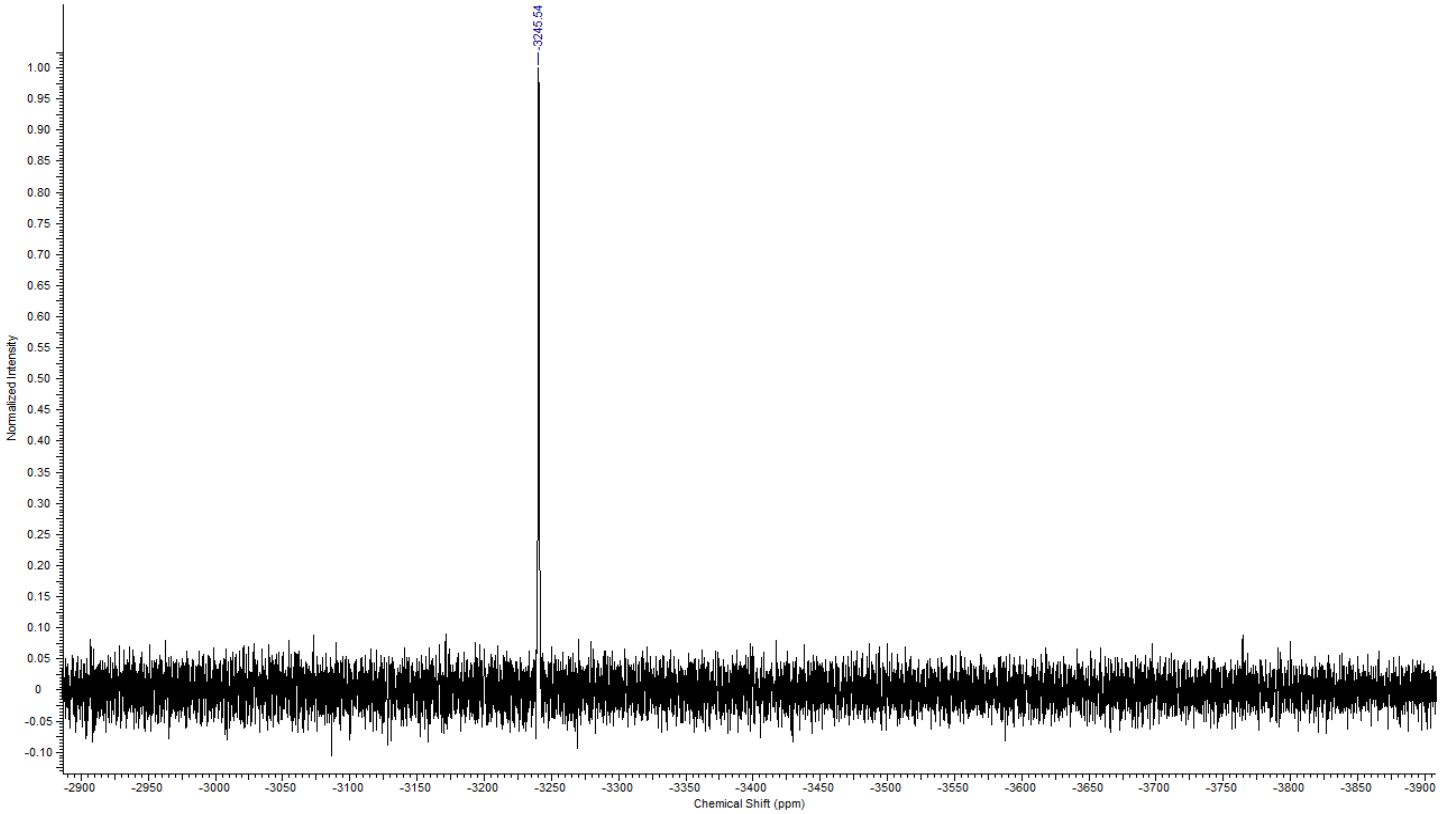

Fig. S 27: ^{195}Pt-NMR spectrum (108 MHz, $CDCl_3$) of complex ***trans*-2c**.

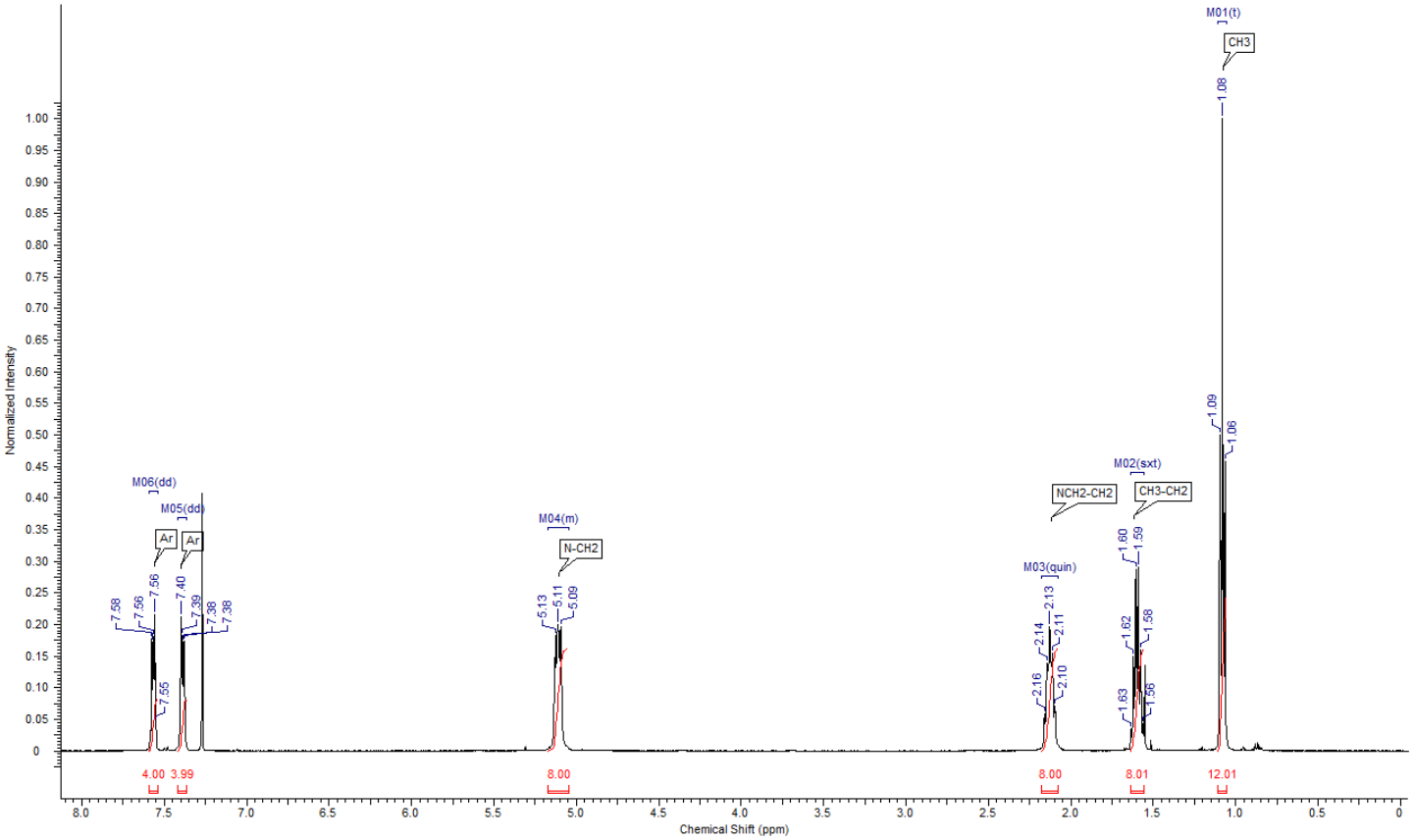

Fig. S 28: ^{1}H-NMR spectrum (500 MHz, $CDCl_3$) of complex ***trans*-4c**.

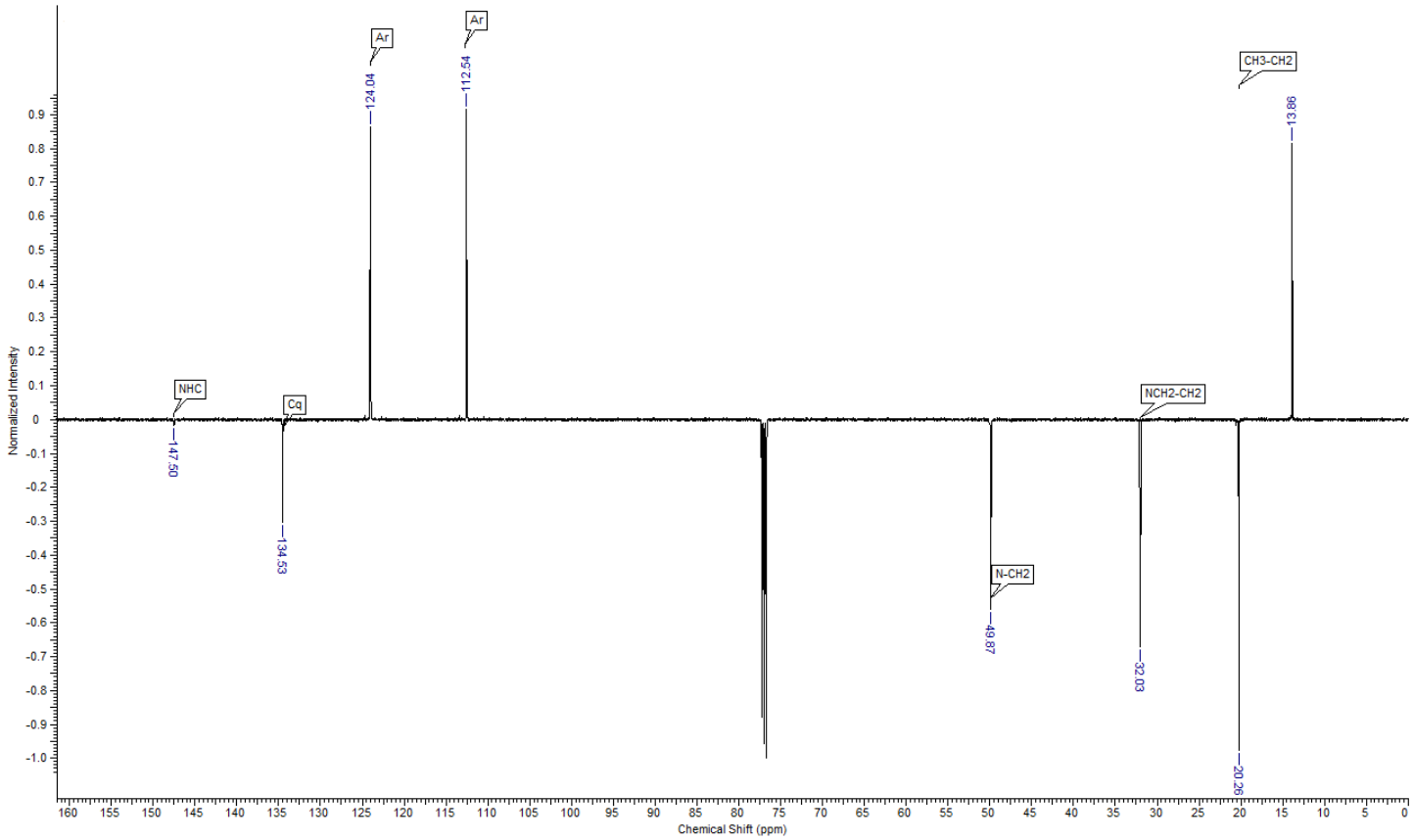

Fig. S 29: ^{13}C-NMR spectrum (126 MHz, $CDCl_3$) of complex ***trans*-4c**.

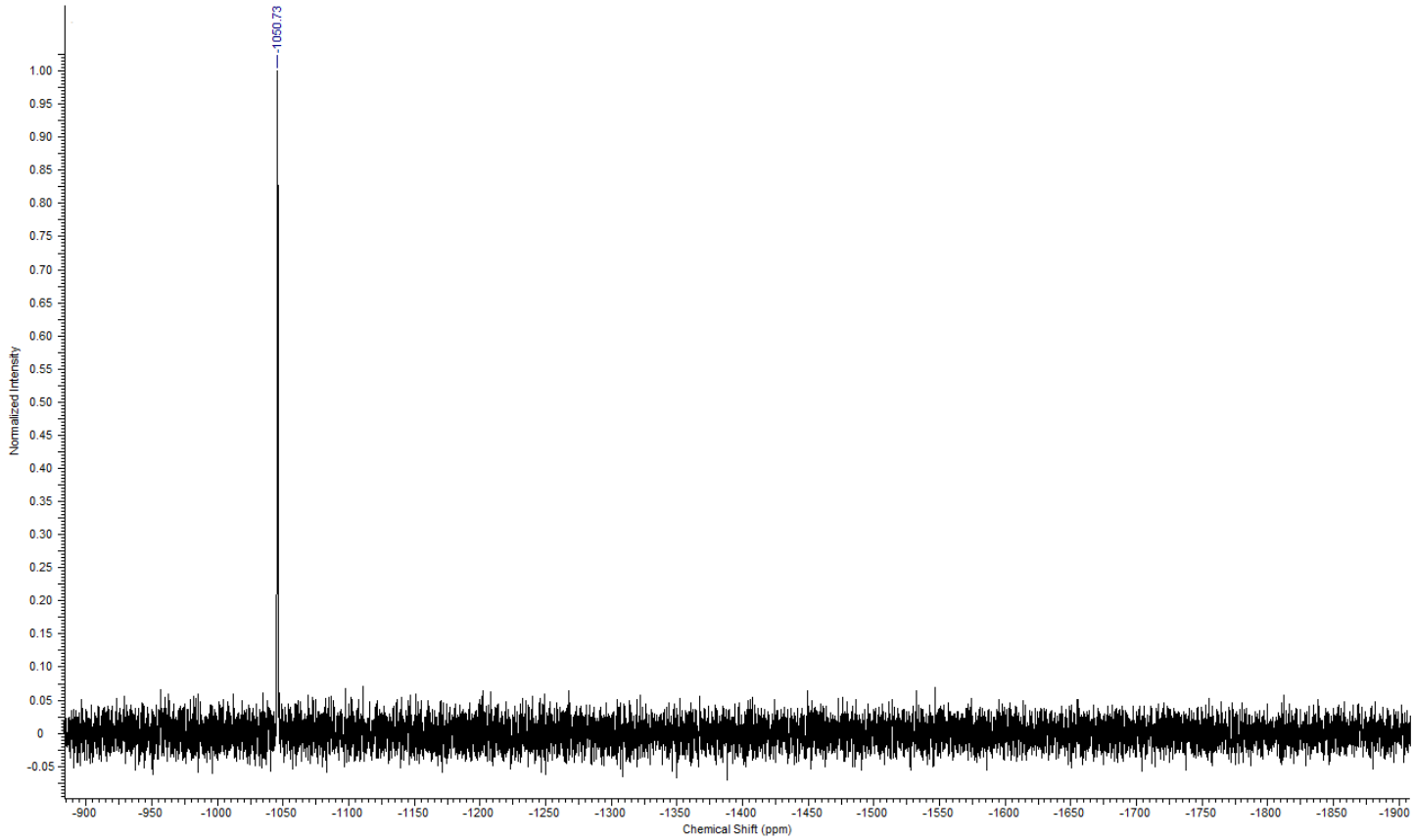

Fig. S 30: ^{195}Pt-NMR spectrum (108 MHz, $CDCl_3$) of complex ***trans*-4c**.

Oxidation of complex 2b with NaOCl

Pt^{IV} hydroxo complexes with NHC ligands have not been published yet.

Upon treating benzylated complex **1** with H_2O_2, a new ^{195}Pt NMR signal around -855 ppm ($CDCl_3$) arose but the reaction was never completed and at the same time accompanied by decomposition due to cleavage of the benzyl group forming benzoic acid.

H_2O_2 oxidation of the *N*-alkylated benzimidazole-2-ylidene complexes **2** afforded only starting material even with a vast excess of peroxide (H_2O_2 or ^{t}BuOOH) at elevated temperatures.

By treating **2b** with NaOCl in water/acetonitrile a new compound with a ^{195}Pt NMR signal at about -905 ppm ($CDCl_3$) appeared, but like before, neither did the reaction go to completion nor was it possible to separate any products from residual starting materials.

In one such run, crystals of a reaction product precipitated from $CDCl_3$ in the NMR tube. NMR spectra of freshly prepared solutions of these crystals in DMSO-d_6 were in agreement with the tentative structure **8** although alternative structures cannot be excluded with certainty. The same sample five days later showed only signals of pure starting Pt^{II} complex **2b**.

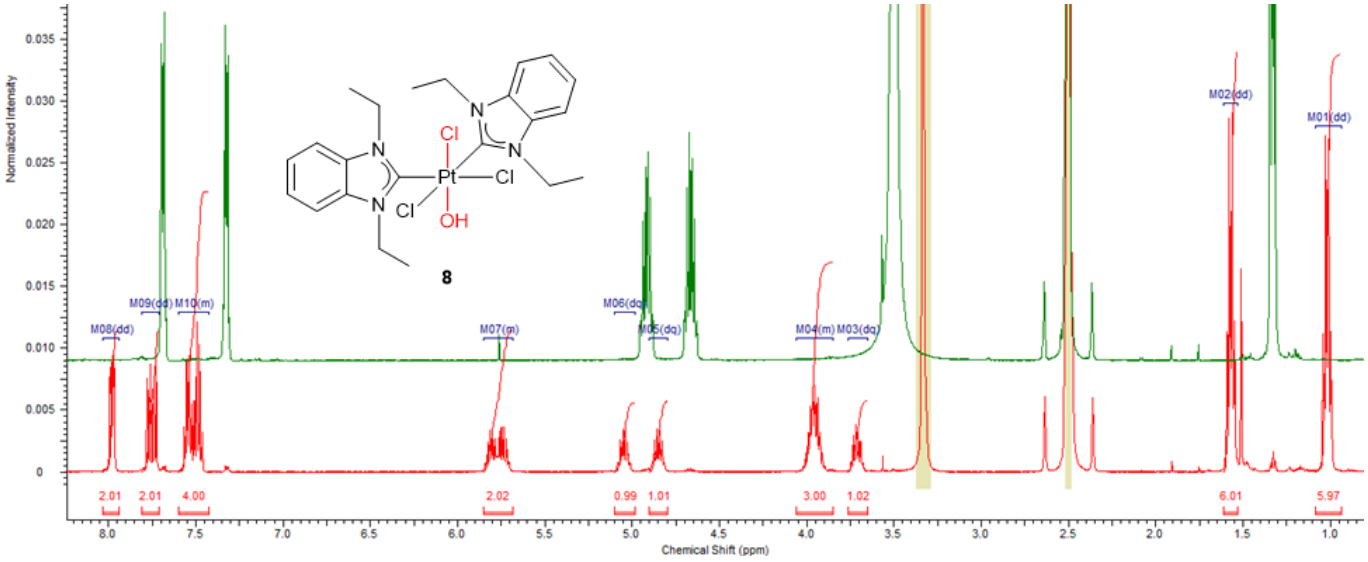

Fig. S 31 red: ^{1}H NMR (DMSO-d_6) of purported Pt^{IV} hydroxo complex **8** with characteristic signals of individual N-CH_2 protons between 3.5 and 6.0 ppm caused by inequivalent axial ligands;
green: same sample five days later shows spectrum of starting Pt^{II} complex **2b**.

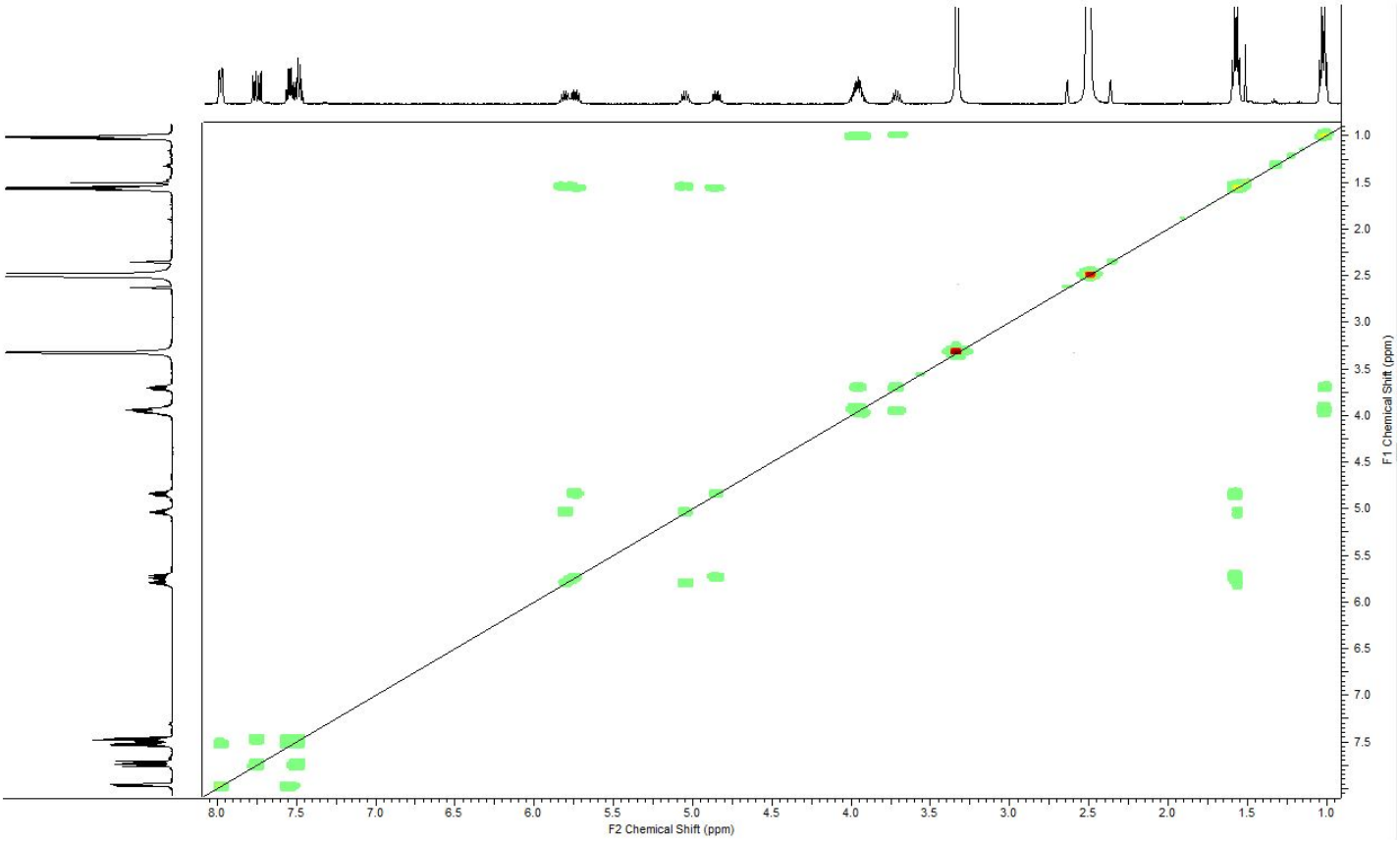

Fig. S 32 COSY-Spectrum of compound **8** in DMSO-d_6

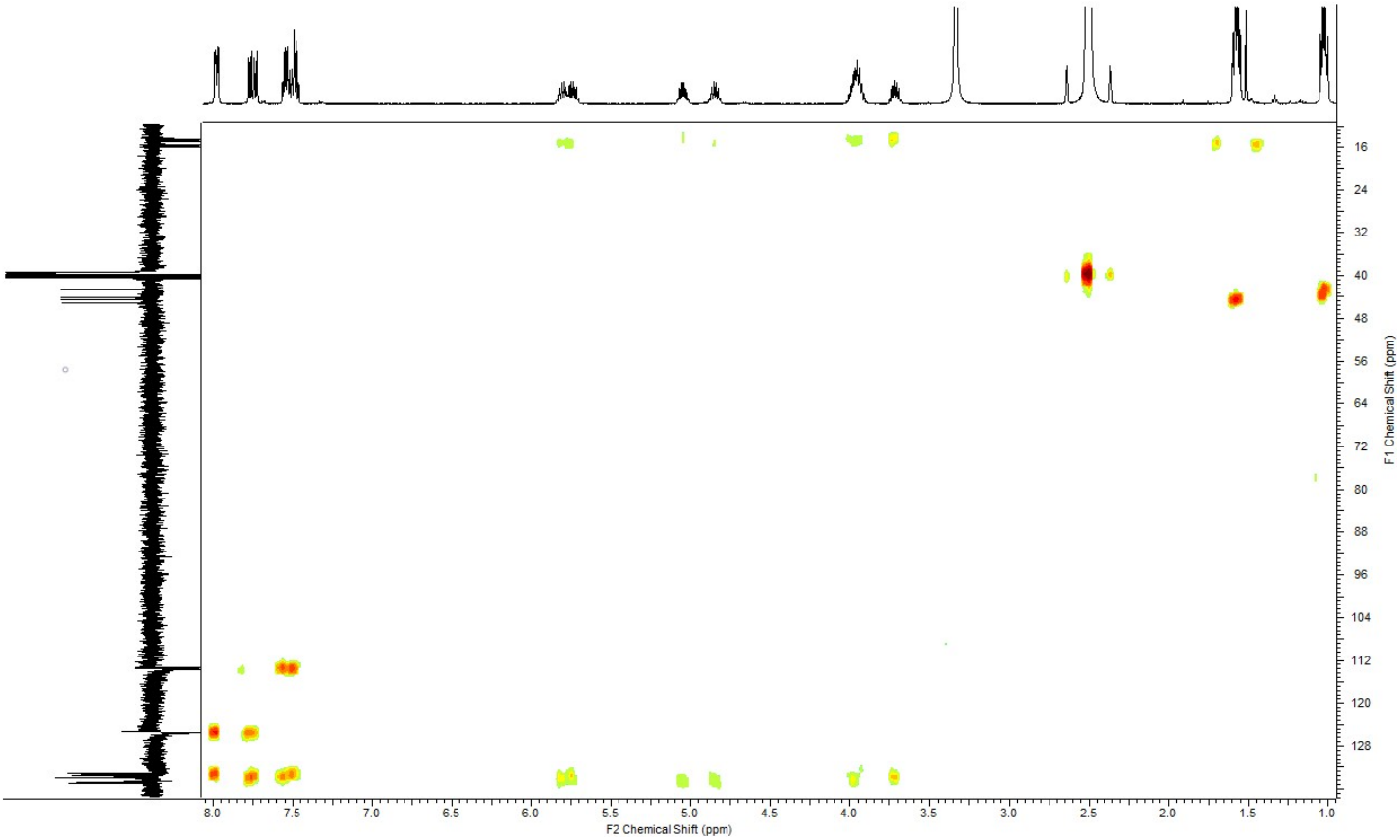

Fig. S 33 HMBC-Spectrum of compound **8** in DMSO-d_6

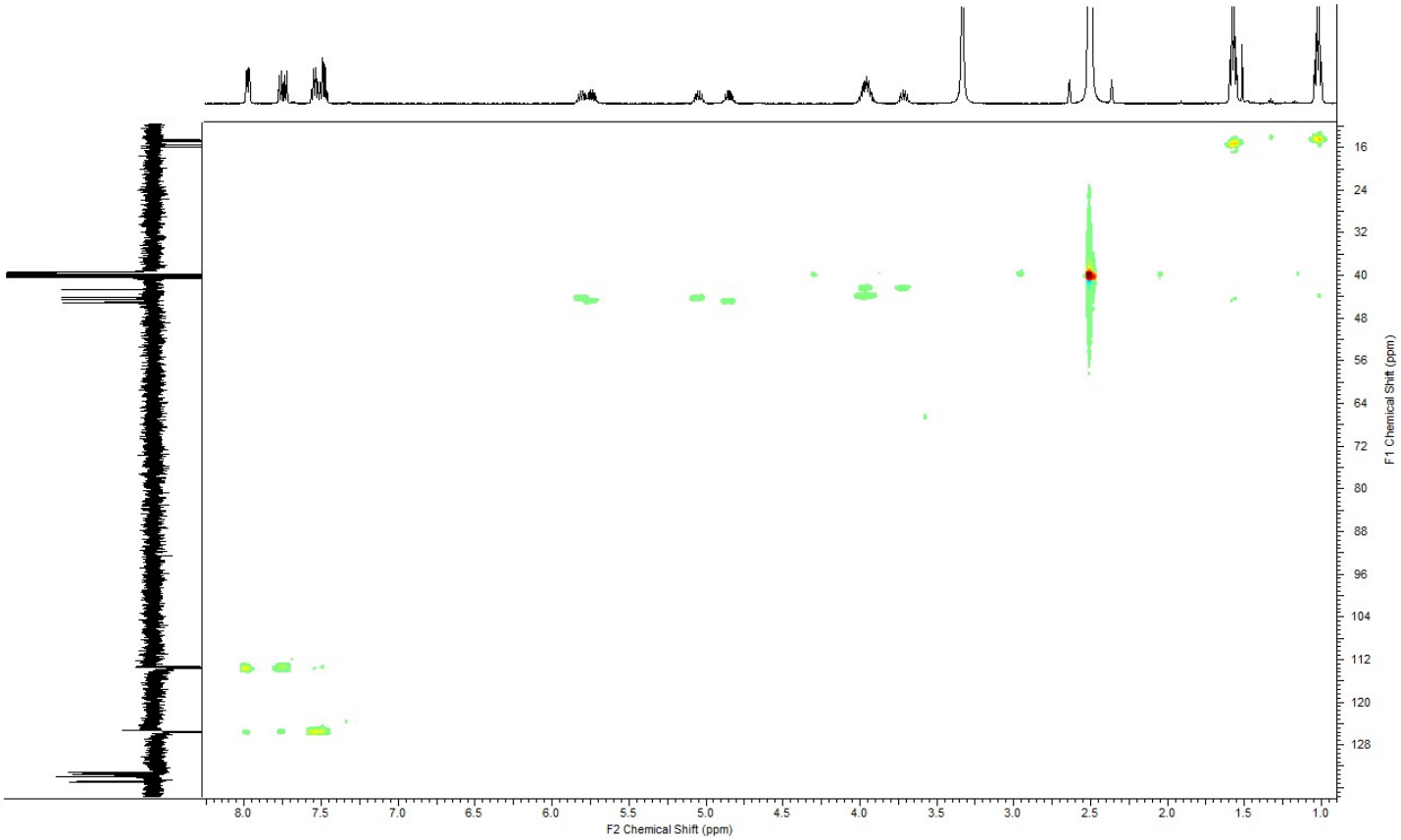

Fig. S 34 HSQC-Spectrum of compound **8** in DMSO-d_6

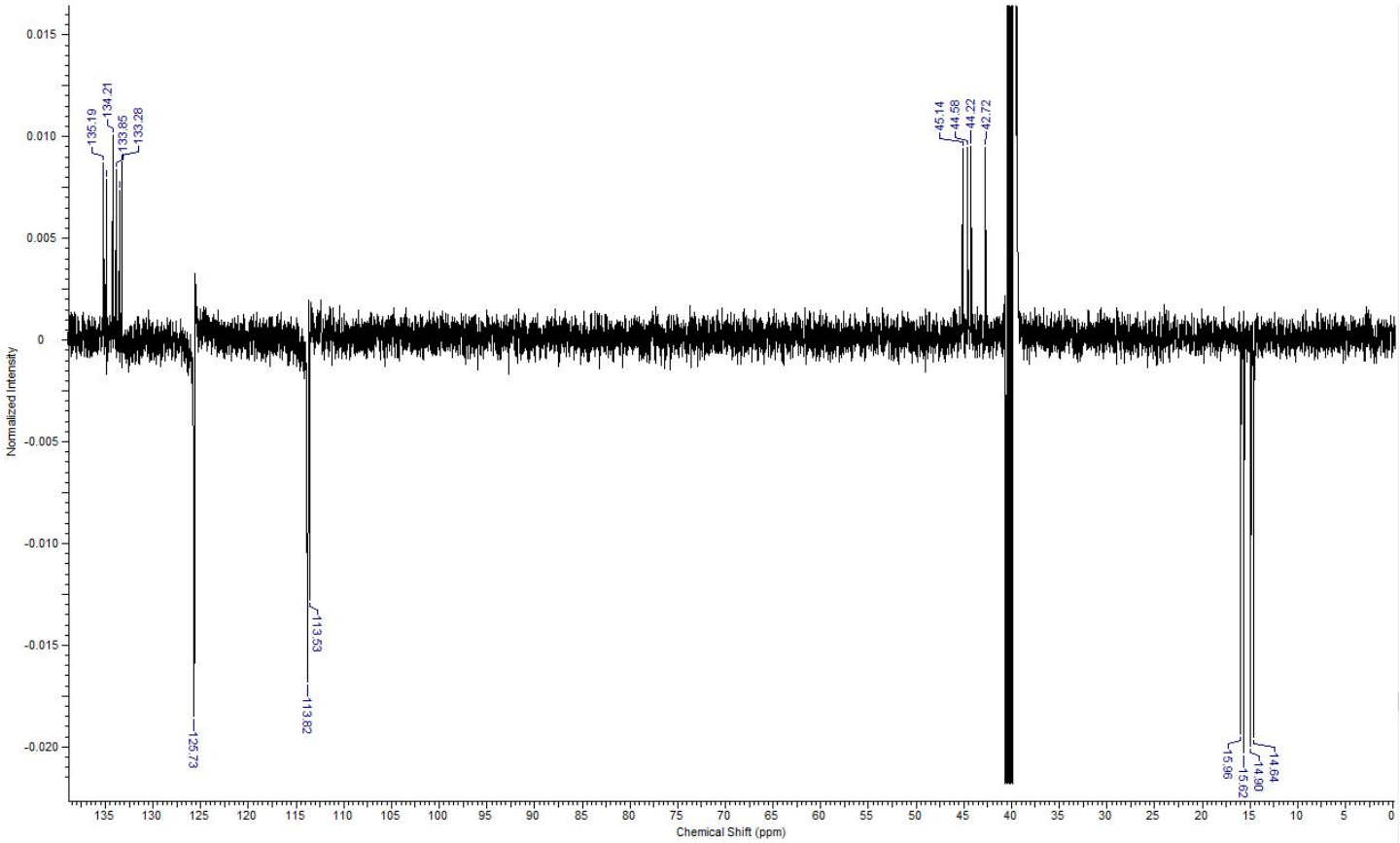

Fig. S 35 JMOD-Spectrum of compound **8** in DMSO-d_6

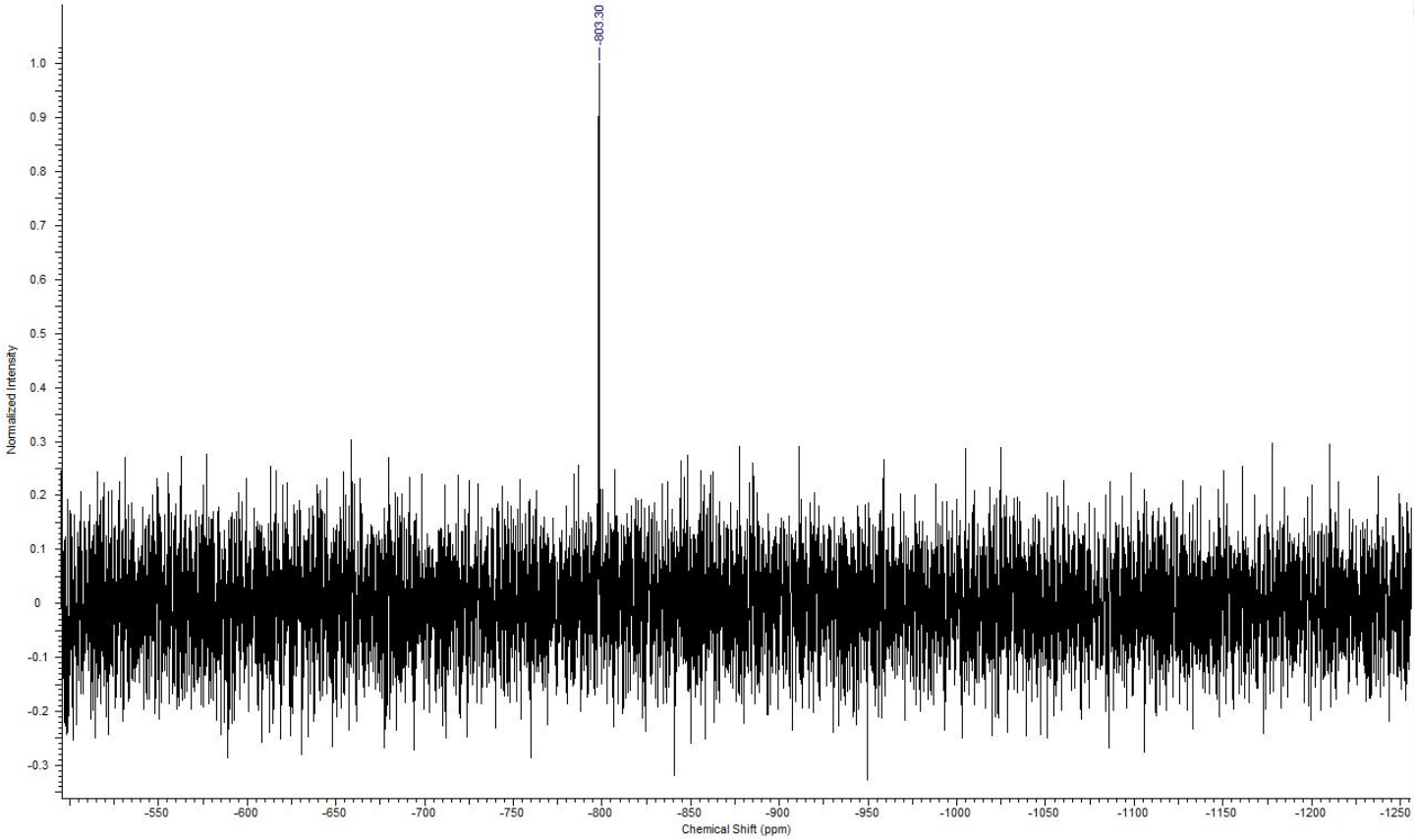

Fig. S 36 ^{195}Pt-Spectrum of compound **8** in DMSO-d_6

Stability of complex 4b in DMSO / water

UV/vis spectra (Fig. S 37): were recorded of 2 mL of a 25 µM solution of complex **4b** (from a 5 mM stock solution in DMSO) in water/DMSO (4:1) over a period of 24 h (every 5 min for the first 3 h) by means of a Cary 60 UV-Vis Spectrometer (Agilent Technologies). Absorptions are relative to a baseline set to 0 at 400 nm.

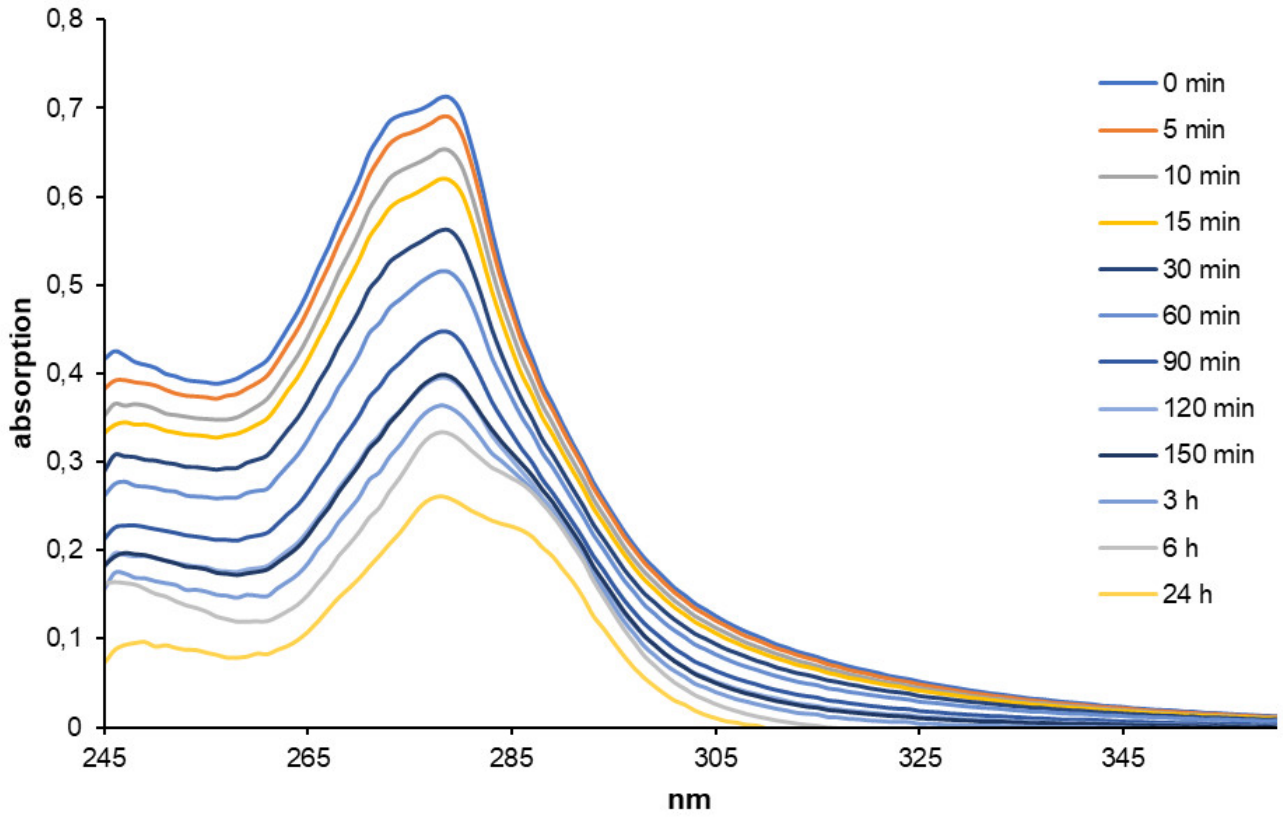

HPLC–ESI mass spectra: were recorded on a Varian 1200 Quadrupole MS/MS spectrometer of diluted NMR solutions of complex **4b** in water / DMSO-d_6 (30:70) after 0 min, 5 min, 10 min, 15 min, 30 min, 1 h, 2 h, and 16 h. The area of the total ion current (TIC) filtered for the main decomposition species with m/z = 579 was calculated for each of these points in time.

Exemplary MS after 10 min:

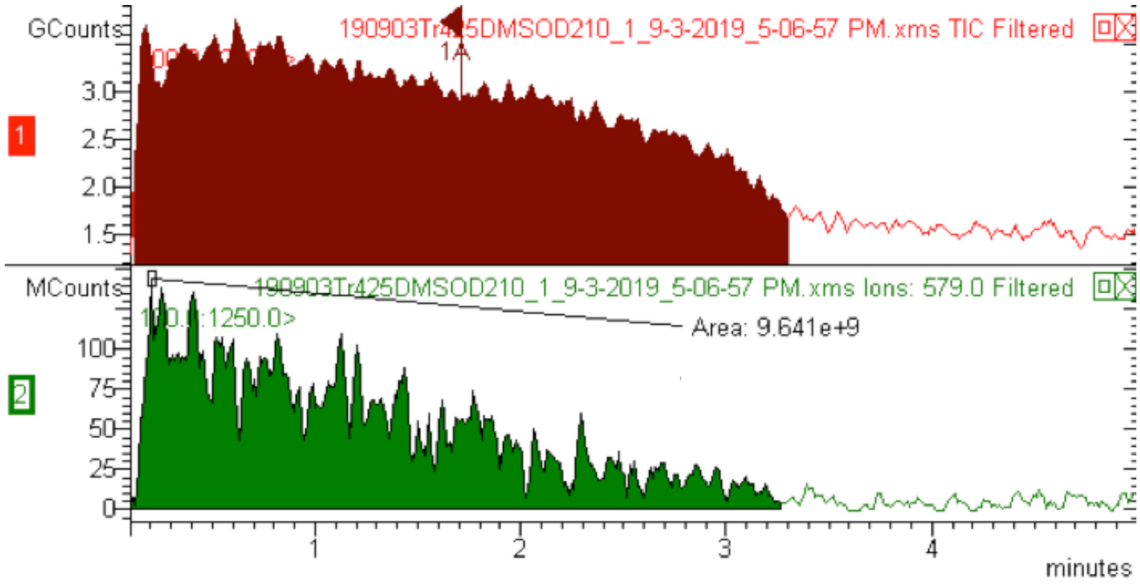

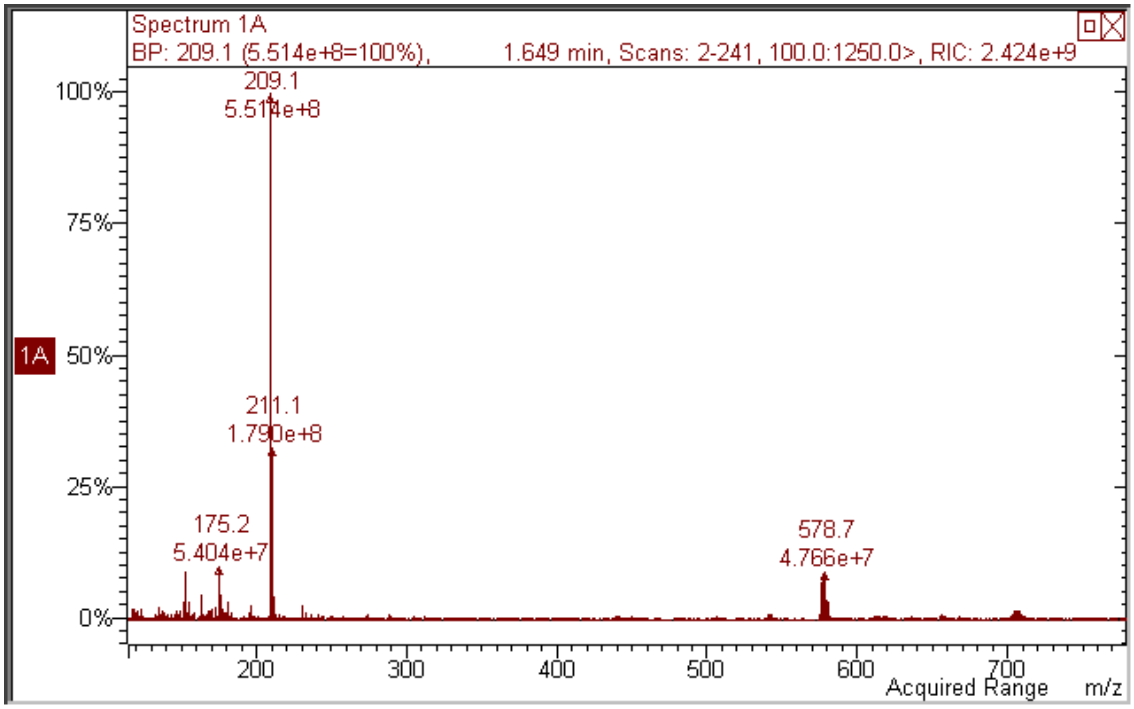

Fig. S 38: 1. Top in red: TIC = Total Ion Current from 0-3.2 min;
2. Middle in green: peak m/z = 579 integrated from 0-3.2 min to give an area of 9.641×10^9
3. Bottom: spectrum 1A, pertinent to TIC from 0-3.2 min.

Exemplary MS after 16 h:

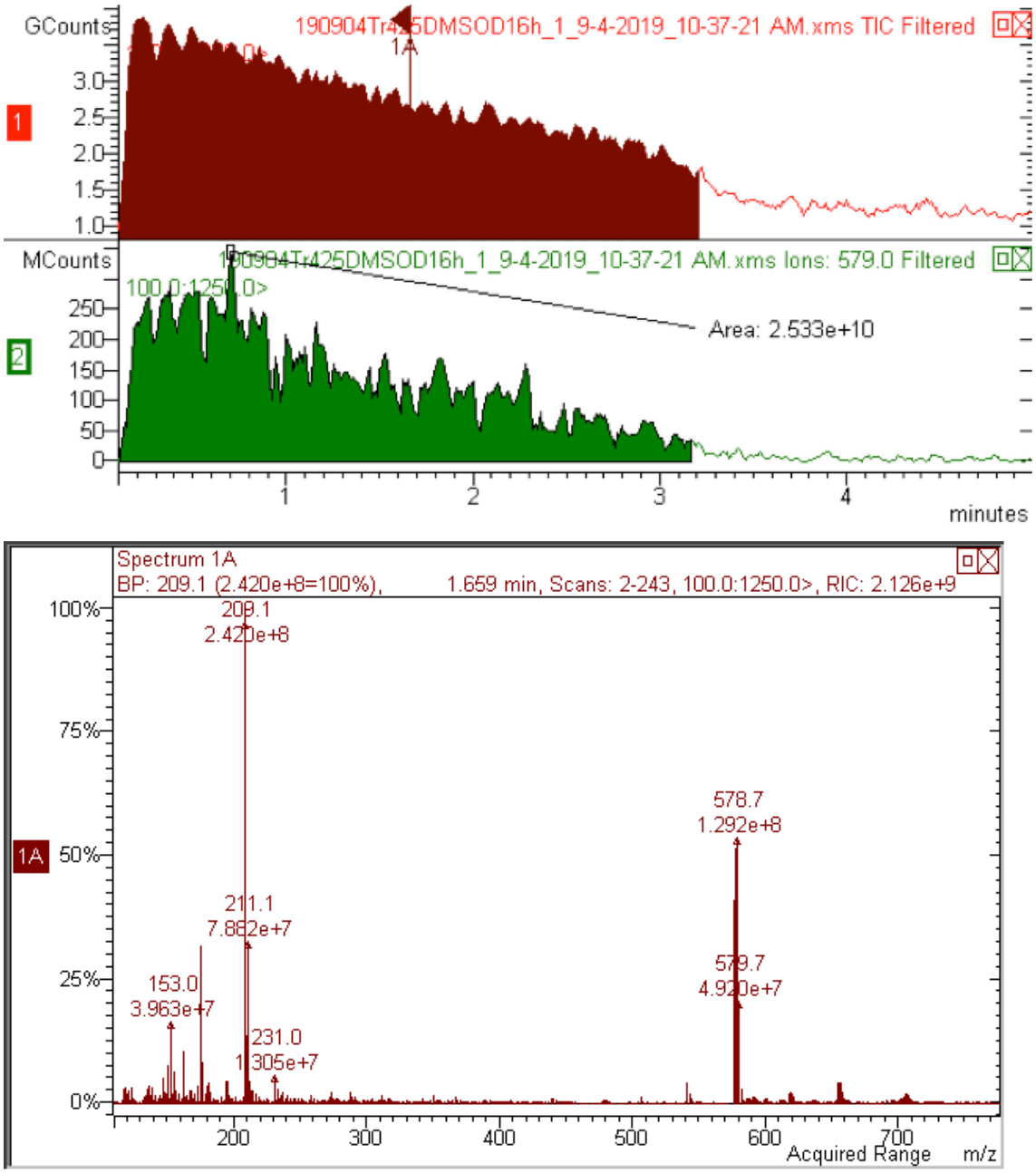

Fig. S 39: 1. Top in red: TIC = Total Ion Current from 0-3.2 min;
2. Middle in green: peak m/z = 579 integrated from 0-3.2 min to give an area of 2.533×10^{10}
3. Bottom: spectrum 1A, pertinent to TIC from 0-3.2 min.

Integration of peak m/z = 579 in spectra from 0-3.2 min recorded over time:

Time	*Area*
0 min	5.35×10^{9}
5 min	8.6×10^{9}
10 min	9.64×10^{9}
15 min	1.08×10^{10}
30 min	1.26×10^{10}
1 h	1.42×10^{10}
2 h	1.8×10^{10}
16 h	2.53×10^{10}

Confirmative MTT-assays with compounds 2c and 2d: were carried out with cells of the same lines yet of *distinctly different* passage numbers:

Table S 2: Means ± SD of IC_{50} (72 h) values [µM] of complexes **2c** and **2d** in MTT assays against human cancer cell lines[a] as calculated from four independent measurements

compounds	IC_{50} (72h) [µM]	
	2c[10b]	**2d**
[a]**518A2**	2.1 ± 0.3	> 50
[a]**HT29**	10.8 ± 1.0	> 50
[a]**DLD-1**	17.4 ± 1.0	> 50
[a]**HCT116^{wt}**	7.0 ± 0.8	> 50
[a]**HCT116$^{-/-}$**	5.3 ± 0.2	> 50

[a]518A2 – melanoma, HT-29 – colon adenocarcinoma, DLD-1 – Dukes type C colorectal adenocarcinoma, HCT116^{wt} – colon carcinoma (wildtype); HCT116$^{-/-}$ – colon carcinoma (p53 knock-out mutant).